

Original Article

Cite this article: Jenkyns HC and Macfarlane S (2022) The chemostratigraphy and environmental significance of the Marlstone and Junction Bed (Beacon Limestone, Toarcian, Lower Jurassic, Dorset, UK). *Geological Magazine* **159**: 357–371. <https://doi.org/10.1017/S0016756821000972>

Received: 5 March 2021

Revised: 12 July 2021

Accepted: 16 August 2021

First published online: 2 November 2021

Keywords:


Toarcian; isotope stratigraphy; condensed limestone; Wessex Basin

Author for correspondence:

Hugh C. Jenkyns,

Email: hugh.jenkyns@earth.ox.ac.uk

The chemostratigraphy and environmental significance of the Marlstone and Junction Bed (Beacon Limestone, Toarcian, Lower Jurassic, Dorset, UK)

Hugh C. Jenkyns  and Sophie Macfarlane

Department of Earth Sciences, University of Oxford, South Parks Road, Oxford, OX1 3AN, UK

Abstract

Two fallen blocks of the Marlstone and stratigraphically overlying Junction Bed sampled on the beach below Doghouse Cliff in Dorset, UK (Wessex Basin) have been examined for carbon and oxygen isotopes of bulk carbonate as well as for strontium, carbon and oxygen isotopes and Mg:Ca ratios in the contained belemnites. The sequence, which contains most of the Toarcian zones and subzones within a metre or less of grey to yellow to pink, red and brown fossil-rich nodular limestone, is extremely condensed and lithologically similar to pelagic red limestones of the Tethyan Jurassic that are locally mineralized with Fe–Mn oxyhydroxides (e.g., Rosso Ammonitico). Strontium-isotope ratios of the contained belemnites are compatible with existing reference curves and both blocks show a rise to more radiogenic values post-dating the Pliensbachian–Toarcian boundary. The high degree of correlation between the relatively negative carbon and oxygen isotopes of the bulk carbonate is compatible with significant diagenetic overprint, and contrasts with higher carbon-isotope values in coeval condensed coccolith-rich limestones elsewhere. Evidence for the characteristic signature of the Toarcian Oceanic Anoxic Event, as represented by organic-rich sediment, is absent, possibly owing to a stratigraphic gap. Both blocks exhibit abrupt carbon-isotope shifts to lower values, one of which could represent the limbs of an incompletely recorded negative excursion associated with the Toarcian Oceanic Anoxic Event. That the Toarcian Oceanic Anoxic Event was also a significant hyperthermal is illustrated in both blocks by a drop in oxygen-isotope values and rise in Mg:Ca ratios of belemnites close to the base of the Junction Bed in the lowest part of the *serpentinum* zone.

1. Introduction

The Junction Bed (*sensu stricto*), deposited in the Wessex Basin (southern UK) and exposed in cliffs along the Dorset coast (Fig. 1), is so called because, together with the underlying Marlstone Rock Bed, it spans the contact between the Middle and Upper Lias (Pliensbachian–Toarcian boundary). It is stratigraphically extremely condensed, containing obvious hardgrounds, and records most ammonite zones and subzones of the Toarcian: it is typically less than a metre in thickness in coastal outcrops. Lithologically, it comprises grey to yellow, pink to red and brown nodular micritic limestone, fossil-rich and heavily mineralized with dark-coloured iron and manganese oxyhydroxides, locally in the form of centimetre-scale nodules, coatings and dendrites (Buckman, 1922; Jackson, 1922, 1926; Arkell, 1933; Howarth, 1957, 1992; Hallam, 1967; Sellwood *et al.* 1970; Cope *et al.* 1980; Jenkyns & Senior, 1991; Hesselbo & Jenkyns, 1995).

Ammonites, whose shells may be partially eroded or corroded and/or serpulid-encrusted and present as internal moulds, are common in the Junction Bed (*sensu stricto*), as are belemnites. Bivalves, brachiopods, gastropods and nautiloids are accompanying faunal elements (Hallam, 1967; Boomer *et al.* 2009; King, 2011); smaller-scale biota includes foraminifera and ostracods. Calcareous nannofossils are found locally in age-equivalent strata but are not abundant in the outcrops on the Dorset coast (Jenkyns & Senior, 1991; cf. Boomer *et al.* 2021). Cupola-shaped stromatolitic structures are present at some levels (Sellwood *et al.* 1970). In overall appearance, the Junction Bed (*sensu stricto*) closely resembles some of the highly condensed fine-grained pelagic coccolith-rich red limestones of the Tethyan Jurassic (e.g. Rosso Ammonitico) that also commonly contain stromatolites, possibly formed from microbial organisms growing within the photic zone, and mineralized Fe–Mn oxyhydroxide nodules and hardgrounds and which formed on fault-bounded topographic highs or seamounts, typically related to extensional half-graben systems (e.g. Jenkyns, 1970, 1971; Jenkyns & Torrens, 1971; Bernoulli & Jenkyns, 1974; Prescott, 1988; Cronan *et al.* 1991; Vera & Martín-Algarra, 1994; Massari & Westphal, 2011; Reolid, 2011; Föllmi, 2016; Scopelliti & Russo, 2021).

The underlying Marlstone Rock Bed, formerly thought to be entirely of *spinatum* zone age, but now known to include the *tenuicostatum* zone, thereby crossing the Pliensbachian–Toarcian boundary (Arkell, 1933; Howarth, 1980), is a coarse-grained pink to brown conglomeratic

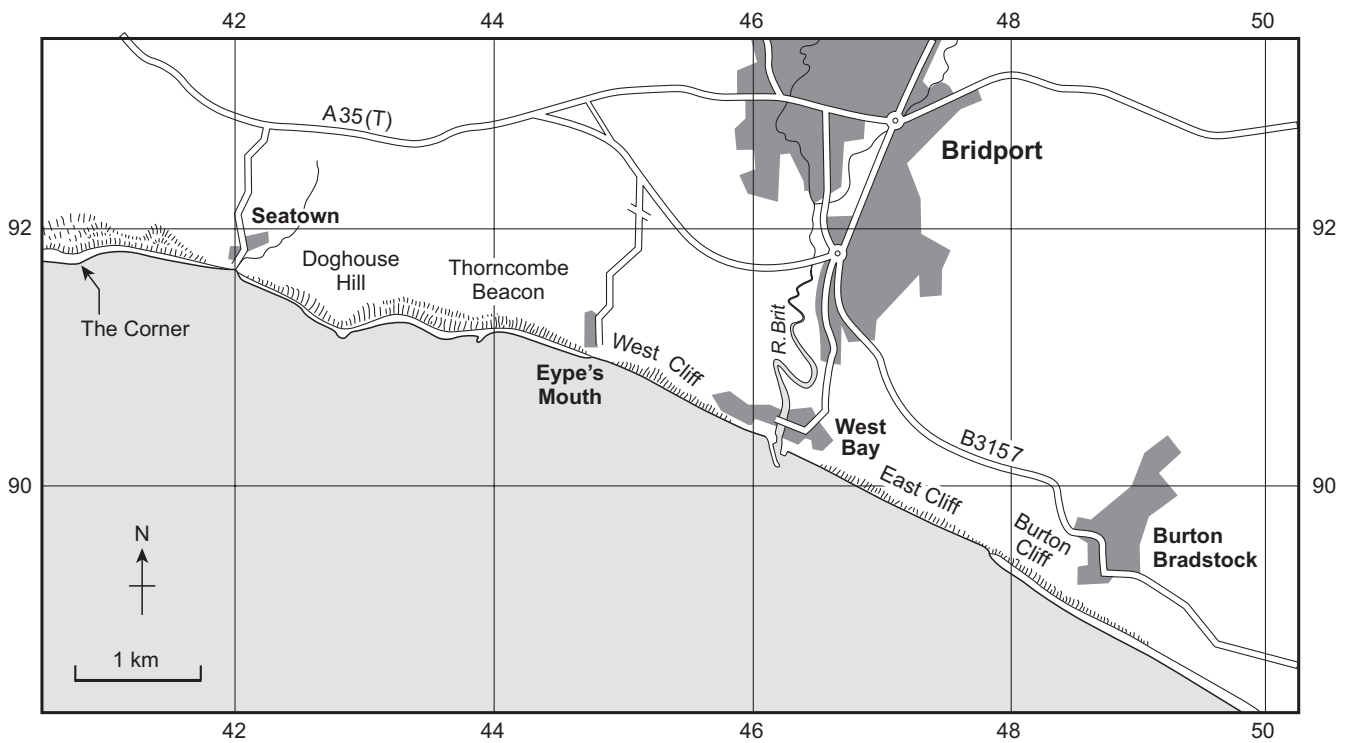


Fig. 1. Map of the Dorset coast, showing the location of Doghouse Cliff, below which blocks of Marlstone and Junction Bed in so-called normal facies are common on the foreshore. Further east, close to where the Eype's Mouth Fault appears in the cliff, so-called fissure facies are present as neptunian sills of graded ammonite-rich micritic limestones that penetrate the Marlstone/Junction Bed complex (Jenkyns & Senior, 1991). The tops of some of the fissure fills contain sparry ferrocalcite (Raven & Dickson, 1989). Modified from Hesselbo & Jenkyns (1995).

crinoidal Fe-oolitic limestone, also relatively condensed being nowhere more than 0.6 m thick, whose biota is similar to that of the overlying Junction Bed (*sensu stricto*), from which it is clearly separable as a distinct lithological unit: the contact between the two units is sharp and marked by an obvious hardground. In the new stratigraphic scheme promulgated by the British Geological Survey, the two units are together referred to as the Beacon Limestone Formation, with the Junction Bed itself (*sensu stricto*) termed the Eype Mouth Limestone (Cox *et al.* 1999). In this account, the original nomenclature, sanctioned by long use, is retained and all subsequent references to the Junction Bed refer only to the fine-grained reddish limestone and do not include the underlying conglomeratic Marlstone, even though it is this unit that is now known to record the stage boundary (Fig. 2).

Significantly, perhaps, given the Tethyan aspect of the Junction Bed, the underlying Marlstone, from which fossils are easier to extract, contains a brachiopod fauna dominated by rhynchonellids with southern European affinities that are otherwise rare in Britain (Ager, 1956). Showing a similar pattern of distribution, and also contained within the Marlstone, are certain gastropods including *Discohelix*, which is locally abundant in exposures in the Alps, Apennines and Sicily (Jackson, 1922, 1926; Hallam, 1967; cf. Wendt, 1968; Conti & Monari, 2003).

Although difficult to access in coastal outcrops, fallen blocks of the Marlstone and Junction Bed can be examined on the foreshore to the east of the hamlet of Seatown in Dorset below Doghouse Hill (Fig. 1) and two such blocks were investigated in this study. Original stratigraphic orientation of the blocks is facilitated by the presence of the characteristic coarse-grained conglomeratic Marlstone welded to the base of the Junction Bed. Detailed study of the Marlstone and Junction Bed by Jackson (1922, 1926) enabled

recognition of a number of distinct layers with characteristic lithology and fauna, labelled with various letters of the alphabet, as illustrated in Figure 2 (Arkell, 1933; Cope *et al.* 1980; Hesselbo & Jenkyns, 1995). The suggested stratigraphy of the two investigated blocks is shown in Figures 3 and 4. It should be noted that age determinations are not constant across the outcrop, a difference that will necessarily be reflected in the sedimentary record of the fallen blocks on the beach.

The Junction Bed contains faunas representing all the zones of the Toarcian from the *serpentinum* (*falciferum*) to the *levesquei*. Significantly, however, the presence of the lower part of the *exaratum* subzone (of the *serpentinum* zone) has never been proven (Howarth, 1992). The time interval represented by the Marlstone and Junction Bed would have been characterized by environmental events around the Pliensbachian–Toarcian boundary including the Toarcian Oceanic Anoxic Event (T-OAE) and associated hyperthermal episode, although the potential of the condensed and incomplete nature of the sequence to capture the signature of these major phenomena is obviously open to question. This matter is addressed in the following account.

It should be noted that the Junction Bed and Marlstone in this area are in so-called 'normal facies' with well-ordered stratigraphy, albeit highly condensed; further to the east, in the proximity of the Eype's Mouth Fault (Fig. 1), the sequence is further complicated by the presence of so-called 'fissure facies' that are represented by out-of-sequence neptunian sills of pale-coloured fine-grained locally ammonite-rich micrite and later void-filling calcite penetrating older grey-green to reddish-brown calcareous/ferruginous/quartz-bearing sedimentary units of the Marlstone–Junction Bed complex (Jenkyns & Senior, 1977, 1991; Raven & Dickson, 1989). The geometry of the multi-generational fissure fills

BIOSTRATIGRAPHY			LITHOSTRATIGRAPHY				LITHOLOGY	
Stages	Zones	Subzones	Nomenclature from Jackson (1922, 1926) Hesselbo and Jenkyns (1995) and Cox <i>et al.</i> (1999)					
TOARCIAN	<i>levesquei</i>	<i>aalensis</i>	I	Junction Bed <i>sensu stricto</i>	Junction Bed <i>sensu lato</i>	BEACON LIMESTONE FORMATION	Red to pink and grey conglomeratic and nodular limestone	
		<i>moorei</i>						
		<i>levesquei</i>						
		<i>dispansum</i>						
	<i>thouarsense</i>	<i>fallaciosum</i>						
		<i>striatulum</i>						
	<i>variabilis</i>							
	<i>bifrons</i>	<i>crassum</i>						K
		<i>fibulatum</i>						L
		<i>commune</i>						M
	<i>serpentinum</i>	<i>falciferum</i>						O + N
<i>exaratum</i>								
<i>tenuicostatum</i>	<i>semicelatum</i>	P	Marlstone					
	<i>tenuicostatum</i>							
	<i>clevelandicum</i>							
	<i>paltum</i>							
PL	<i>spinatum</i>	<i>hawskerense</i>	Px					
		<i>apyrenum</i>	R					
							Grey, argillaceous nodular limestone and marl	
							Grey, pink and brown weakly Fe-oolitic crinoidal limestone	
							Red-brown conglomeratic, Fe-oolitic limestone	

Fig. 2. Litho- and biostratigraphy of the Marlstone and Junction Bed (Junction Bed *sensu lato*), grouped together as the Beacon Limestone by the British Geological Survey (Cox *et al.* 1999). Modified from Hesselbo & Jenkyns (1995). Stratigraphy follows Jenkyns & Senior (1991) and Howarth (1992). The contact between the Middle and Upper Lias (Pliensbachian-Toarcian) was originally thought to lie between the Marlstone and the Junction Bed (hence its name) until discovery of *tenuicostatum* zone ammonites in the highest parts of the stratigraphically lower unit (cf. Arkell, 1933; Howarth, 1980). PL – Pliensbachian.

indicates that this lithological complex was moderately consolidated when syn-sedimentary faulting and sedimentary disruption took place, implying some degree of lithification of the host sediment on or just below the sea floor that pre-dated significant burial. The Eype’s Mouth Fault is but one of a number of active extensional Jurassic faults that characterized the Wessex Basin during a period of active subsidence and suggests that the Marlstone and Junction Bed exposed on the Dorset coast were deposited on the relatively non-subsident part of a tilted block that probably had only modest effect on sea-floor topography but may have extended into the photic zone (probably ~200 m or less), allowing local development of microbially mediated stromatolites (Sellwood & Jenkyns, 1975; Chadwick, 1986; Karner *et al.* 1987; Jenkyns & Senior, 1991; cf. Jenkyns, 1971; Vera and Martin-Agarra, 1994; Massari and Westphal, 2011; Reolid, 2011).

2. Methodology

The two fallen blocks investigated were oriented and described in the field with samples of bulk rock obtained using a cordless drill positioned every centimetre or less and the resultant powder put into sample bags. The tungsten carbide drill bit was cleaned with dilute HCl after each use to avoid cross-contamination. To obtain some primary skeletal calcite, all observed belemnites were collected from the sections using a hammer and chisel.

The powders thus obtained from bulk rock were analysed on a VG Isogas Series Prism Mass Spectrometer at Oxford University for carbon- and oxygen-isotope ratios using standard techniques, as described in Woodfine *et al.* (2008). Analytical reproducibility of replicate standards (Carrara Marble) on the instrument was typically less than 0.1 ‰ for both carbon- and oxygen-isotope ratios.

Belemnites were prepared as in the method of Jones *et al.* (1994) for strontium-isotope analyses, samples of 100–200 mg being first cleaned to remove matrix, crushed and repeatedly etched in

0.3M HCl to remove diagenetic calcite, followed by rinsing in distilled water. Subsequently, some fossil fragments were set aside for carbon- and oxygen-isotope analysis, the rest being dissolved in 6 % HNO₃ (vol.–vol. %) before undergoing further dilution with 1 % HNO₃ and addition of an indium internal standard. Solutions were analysed for a suite of trace and major elements (including Mg, Ca, Mn, Fe) on a Perkin Elmer Sciex Elan 6100 DRC Quadrupole inductively coupled plasma mass spectrometer (ICP-MS) at Oxford University following the technique of Rosenthal *et al.* (1997). Typical analytical uncertainty for Mg/Ca on this instrument, obtained from the standard deviation of a synthetic standard, is ~2.4 % (e.g. Ferguson *et al.* 2008).

Strontium was separated from pre-prepared solutions using standard procedures (Jones *et al.* 1994) and then loaded into a VG Isomass 54E solid-state thermal ionization mass spectrometer (TIMS). Results were normalized to an NIST SRM 987 standard value of 0.710250. The long-term (3 years) average of the standard over the period of analysis was 0.710248 with a 95 % confidence interval (2σ) of 2.6 × 10⁻⁶. All samples contained less than 150 ppm Fe, the cut-off used by Jones *et al.* (1994) to exclude potentially altered fossils likely to give elevated strontium-isotope ratios and plot above the reference curve. The only belemnite with an Fe value in excess of 100 ppm, which also has an anomalous Mn value of 965 ppm, is at the 20 cm level in Block 2.

The data generated (carbon- and oxygen-isotope ratios of bulk carbonate and belemnites, strontium-isotope ratios of belemnites, Mg:Ca ratios of belemnites) have been plotted against the lithological log of the Marlstone and Junction Bed (Figs 5, 6).

3. Chemostratigraphic data

3.a. Carbon isotopes in bulk carbonate

In Block 1, the bulk carbon-isotope ratios in the Marlstone, of *spinatum*–*tenuicostatum* zone age, are relatively low, with most

Block 1

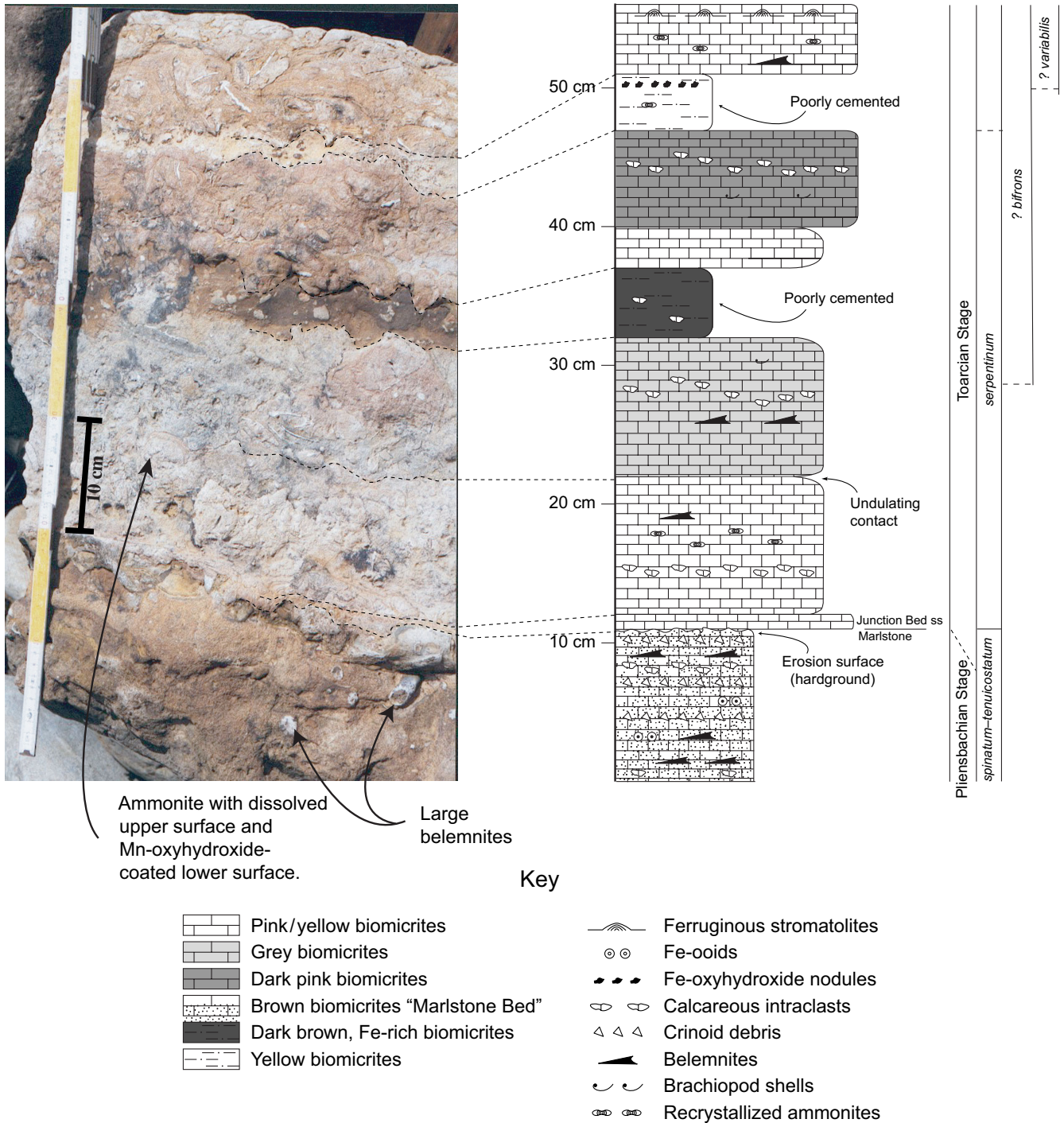


Fig. 3. (Colour online) Field aspect of Block 1, showing the contact between the Marlstone and the overlying Junction Bed (*sensu stricto*). Biostratigraphy is interpretative. Ammonite zones in italics.

values falling between -4‰ and -3‰ (Fig. 5). There is an abrupt shift across the contact with the overlying finer grained Junction Bed where values are consistently higher, generally in the range $1\text{--}2\text{‰}$. Such values persist up to the half-way level of the Junction Bed, of probable *serpentinum* zone age, where there is a pronounced negative excursion with values falling to $\sim -6\text{‰}$ at around the 33–35 cm level. Following recovery from this

negative shift, values return to background levels of $1\text{--}2\text{‰}$. Close to the top of the block, values fall again with a minimum figure of -1.2‰ present at one level before recovering somewhat in the three highest samples.

A similar range of carbon-isotope values is present in Block 2 but the pattern is slightly different in that there is a negative excursion within the Marlstone interval from a background of

Block 2

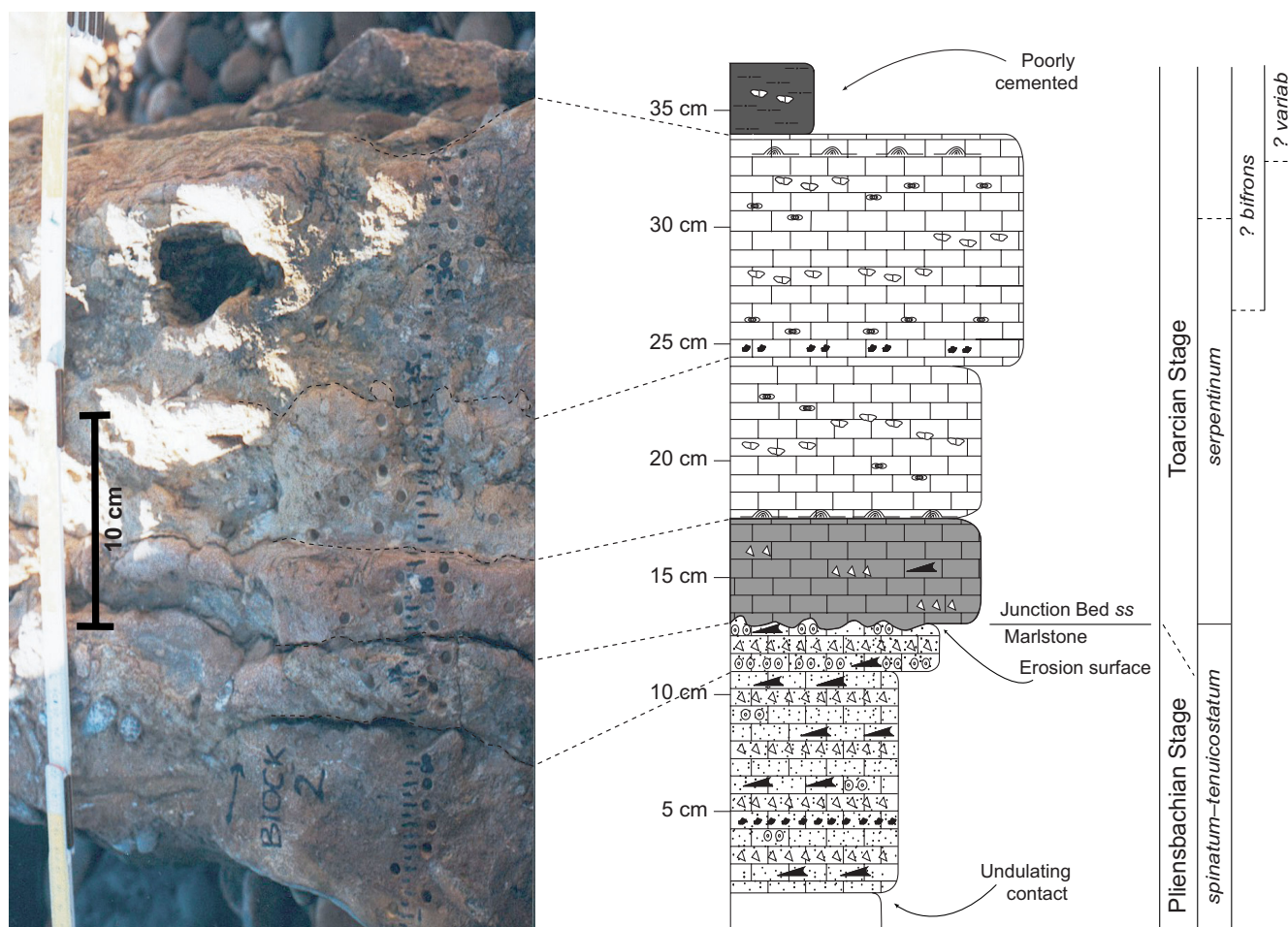


Fig. 4. (Colour online) Field aspect of Block 2 (post-drilling), showing the contact between the Marlstone and the overlying Junction Bed (*sensu stricto*). Biostratigraphy is interpretative. Key as in Figure 3. Ammonite zones in italics. *variab* – *variabilis*.

~–2 to ~–3 ‰ down to –4.5 ‰ before a rise up to just below the contact with the Junction Bed with values in the range 1–1.5 ‰ (Fig. 6). Stratigraphically higher background values in the Junction Bed are similar to those in Block 1 but there are also two negative excursions down to ~–2 ‰ at around the 10–13 cm and 24–25 cm levels, both likely localized in the *serpentinum* zone: these values are considerably less negative than the lowest values seen in Block 1.

In a coeval section, a little more stratigraphically expanded than the sequences exposed on the Dorset coast (as exemplified by Blocks 1 and 2), and cropping out some 30 km to the northeast in Somerset (Preston Plunknett, near Yeovil), the carbon isotopes rise from a background value of between –0.5 ‰ and 0 ‰ in the Marlstone (*spinatum*–*tenuicostatum* zones) to a maximum of >3 ‰ in the lower part of the *serpentinum* zone of the Junction Bed before declining through the *bifrons* zone ultimately into the *thouarsense* zone (Jenkyns & Clayton, 1997). Such isotopic values are in general a little higher than those found in Blocks 1 and 2.

3.b. Carbon isotopes in belemnites

Carbon isotopes of the belemnites in Block 1 show little variation, apart from a minor excursion at around the 15 cm level, with most

values falling in the range 1 ‰ to 3 ‰: figures that in most, but not all cases are higher than values from the enclosing bulk carbonate (Fig. 5). Belemnite values in Block 2 are similar (Fig. 6).

3.c. Oxygen isotopes in bulk carbonate

In Block 1, bulk oxygen-isotope ratios are relatively constant in the Marlstone at around –3 ‰ (Fig. 5). Following this, apart from one anomalously low value, there is a step up across the contact with the Junction Bed to around –1 ‰ followed by a drop back to ~–2 ‰, and such values then generally increase in progressively higher levels towards –1 ‰, punctuated by a distinct negative excursion in the putative *serpentinum* zone where values drop to ~–4 ‰ at around the 33–35 cm level. These low values correlate with low values in the carbon-isotope profile and, in the higher stratigraphic values of the block, the oxygen and carbon isotopes also move in parallel, including the top four values that depart from the overall trend.

Across Block 2, the bulk oxygen-isotope profile also closely matches that of the carbon isotopes (Fig. 6). Overall, against a background of ~–2 ‰, there are three negative excursions with values falling to ~–3.5 ‰ in the Marlstone (*spinatum*–*tenuicostatum* zones) and to ~–3.8 ‰ and ~–2.5 ‰

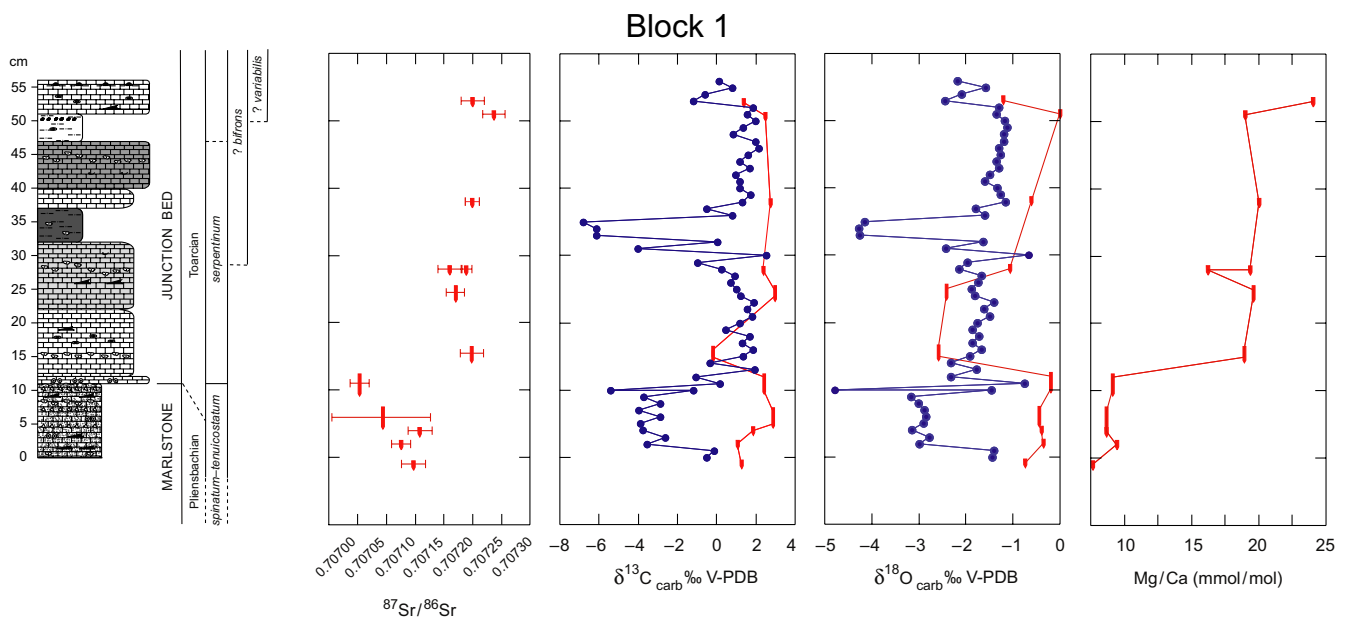


Fig. 5. (Colour online) Chemostratigraphy of Block 1. Note the close correspondence between the carbon- and oxygen-isotope profiles, compatible with a significant diagenetic overprint in the Marlstone and Junction Bed. The strontium-isotope ratios ($^{87}\text{Sr}/^{86}\text{Sr}$) of the belemnites conform to global trends; the oxygen-isotope patterns and Mg:Ca ratios indicate the onset of the Toarcian hyperthermal across the Pliensbachian–Toarcian boundary. Solid circles indicate samples of matrix; vertically oriented bullet-shaped symbols of variable length denote belemnites and the thickness of strata in which the fossils were found. Strontium-isotope error bars are 2σ . Ammonite zones in italics.

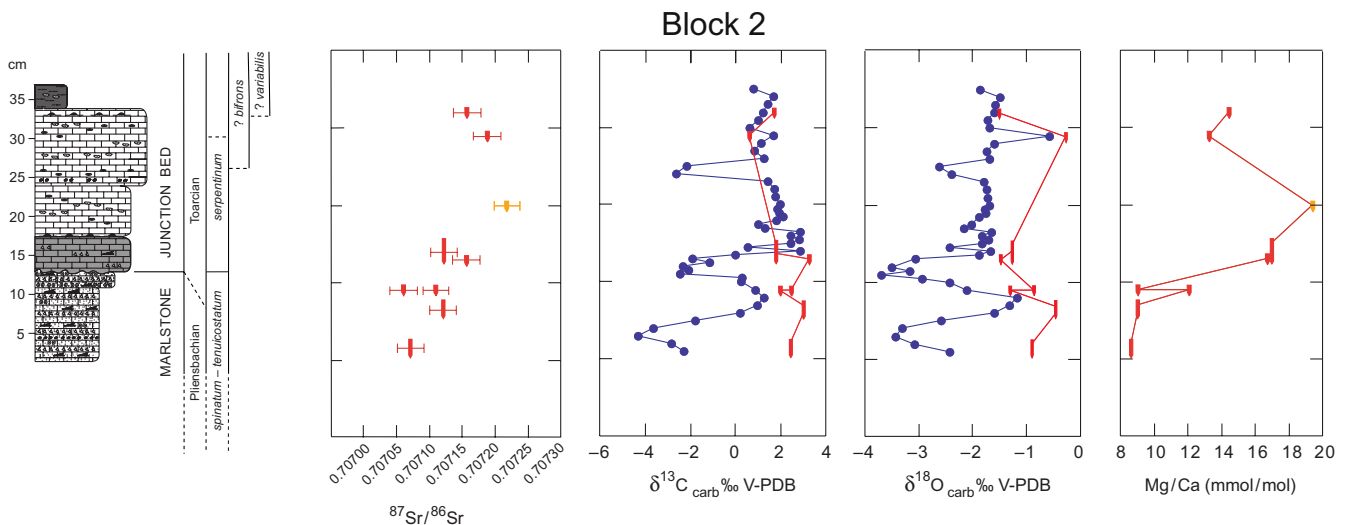


Fig. 6. (Colour online) Chemostratigraphy of Block 2. Note the close correspondence between the carbon- and oxygen-isotope profiles, compatible with a significant diagenetic overprint in the Marlstone and Junction Bed. The strontium-isotope ratios of the belemnites generally conform to global trends although the two, stratigraphically highest samples could be reworked. The belemnite at the 20 cm level (coloured orange) contains elevated contents of Fe and Mn and is considered to be diagenetically compromised and not reliable as a chemostratigraphic index as regards $^{87}\text{Sr}/^{86}\text{Sr}$ and Mg:Ca. The oxygen-isotope patterns and Mg:Ca ratios indicate the onset of the Toarcian hyperthermal across the Pliensbachian–Toarcian boundary, particularly clearly in the case of the latter proxy, whose profile resembles that seen in Block 1. Solid circles indicate samples of matrix; vertically oriented bullet-shaped symbols of variable length denote belemnites and the thickness of strata in which the fossils were found. Strontium-isotope error bars are 2σ . Ammonite zones in italics.

at the 10–13 cm and 24–25 cm levels, respectively in the overlying putative *serpentinum* zone in the Junction Bed itself.

3.d. Oxygen isotopes in belemnites

The oxygen isotopes in the belemnites in Block 1 (Fig. 5) fall between 0 ‰ and –1 ‰ in the Marlstone, followed up-section by a dramatic fall of ~2 ‰ crossing into the basal Junction Bed. Values become generally heavier thereafter in higher levels, albeit

remaining relatively low in the putative *serpentinum* zone. The major drop in oxygen-isotope values of belemnites correlates with an increase in Mg/Ca ratios in the same fossils.

Oxygen-isotope values in the belemnites over the whole of Block 2 (Fig. 6) are mostly around –1 ‰ and are characterized by a ~1 ‰ drop over the Marlstone–Junction Bed contact where the belemnite abundance tolerably well defines the trend. This interval correlates with an increase in belemnite Mg:Ca, as is the case for Block 1.

3.e. Strontium isotopes in belemnites

In Block 1 (Fig. 5), strontium-isotope ratios ($^{87}\text{Sr}/^{86}\text{Sr}$) in belemnites from the Marlstone (*spinatum*–*tenuicostatum* zones) show a subdued decline from 0.707097 to 0.707003 before rising abruptly in the base of the Junction Bed to 0.707198, and similar values persist to the top of the section with the highest figure obtained of 0.707237 in the putative *bifrons*–*variabilis* zones. Two separate belemnites at the 28 cm level give values of 0.707161 and 0.707189.

The pattern in Block 2 (Fig. 6) is not as clear-cut but, again, there are higher values within belemnites from the Junction Bed than those in the Marlstone. Values within the Marlstone fossils fall within the range 0.707072 to 0.707121 and two separate belemnites at the 9 cm mark have values of 0.707061 and 0.70711. At the level of its contact with the Junction Bed, belemnite values increase to the 0.707122–0.707156 range. Stratigraphically above, values rise to a maximum of 0.707218 with the sample at the 20 cm level, this being the belemnite with the highest concentrations of Fe and Mn, before illustrating a gentle decline.

3.f. Mg:Ca ratios in belemnites

In both Blocks 1 and 2, there is a dramatic increase in belemnite Mg:Ca ratios across the Marlstone–Junction Bed contact (Figs 5, 6). Values rise from a general background of ~8–10 mmol/mol to mostly in the range of 18–20 mmol/mol. In Block 1, the highest value is at the top of the section (~24 mmol/mol), lying in the putative *bifrons*–*variabilis* zones. In Block 2, the highest value (21.6 mmol/mol) is at the 20 cm mark in the putative *serpentinum* zone, but it should be noted that this sample has elevated levels of Fe and Mn. In Block 1, the major rise in Mg:Ca ratios of belemnites correlates with a dramatic decrease in oxygen-isotope ratios in the same fossils, a relationship also seen in Block 2. This correlation extends to the strontium-isotope profiles whose belemnites show an abrupt rise at the same level, most obviously displayed in Block 1 (Fig. 5). The apparent synchronous nature of these different geochemical signals is probably an artefact of the extremely condensed nature of the Junction Bed and presumably the underlying Marlstone.

4. Discussion

4.a. Strontium-isotope stratigraphy

The chemostratigraphic significance of strontium-isotope ratios in belemnites can be prone to error. In their detailed study of Lower Jurassic condensed pelagic limestones from the Subbetic Zone of southern Spain, Nieto *et al.* (2008) illustrated instances where the strontium-isotope age of the belemnites, as defined by a high-resolution reference curve (e.g. Jones *et al.* 1994; McArthur *et al.* 2000, 2001; Jenkyns *et al.* 2002), departs from the biostratigraphical age given by the associated ammonites. It seems that, in settings of particularly slow net deposition, relatively robust belemnites can undergo selective reworking up-section owing to winnowing of accompanying sediment and/or bioturbation. Such derived faunas (unaccompanied by coeval more fragile and easily dissolved ammonites) hence give a greater age than does the ultimately entombing sediment and contained younger ammonites. The reverse can also occur, in which case it may be the ammonites, commonly coated with a protective veneer of iron-manganese oxyhydroxides, that are reworked and give the greater age. It is also possible that belemnites can become cemented to the sea floor during hardground formation and, because there is

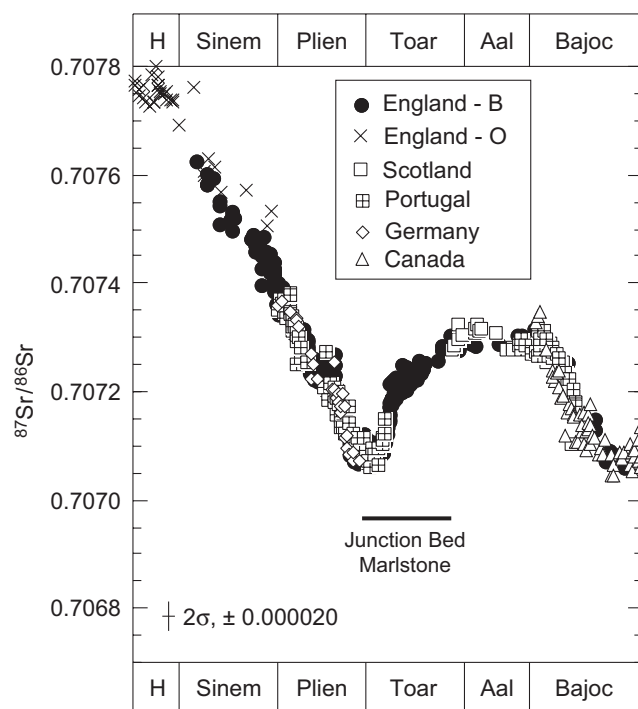


Fig. 7. Strontium-isotope reference curve based on diagenetically screened belemnites from diverse localities except for the ‘England - O’ data points that indicate non-screened oysters as the source of skeletal calcite (after Jenkyns *et al.* 2002). Stratigraphical extent of the Marlstone and Junction Bed, from the *spinatum* to the *levesquei* zone, derives from ammonite determinations (Cope *et al.* 1980; Jenkyns & Senior, 1991; Howarth, 1992). Note the strontium-isotope minimum close to the Pliensbachian–Toarcian boundary, followed by the subsequent rise to progressively more radiogenic values up to the Aalenian, trends most clearly seen in Block 1 (Fig. 5). Together, belemnites from the Marlstone and Junction Bed record this major change in the balance between continental and mantle (mafic) sources of strontium to the world ocean, with increase in the former potentially linked to accelerated weathering of the land surface due to the high global temperatures of the Toarcian hyperthermal. All strontium-isotope data are normalized to a value of 0.710250 for the NBS 987 standard. Duration of stages is plotted according to the number of subzone units (Jones *et al.* 1994).

no net deposition for some while, when ammonite-bearing sediment finally does accumulate it is younger than the belemnites that it encloses. The highly condensed nature of the Junction Bed makes it likely that some or all of these processes may have operated during the Toarcian, thereby compromising to some extent the use of strontium-isotope stratigraphy of the belemnites as a dating tool. Some level of diagenetic modification is possible for all belemnites sampled, a process that in general will tend to move the strontium-isotope ratios to more radiogenic values, thereby confounding their stratigraphic significance to some extent (Jones *et al.* 1994).

These potential complications notwithstanding, it is apparent that the strontium-isotope ratios in both blocks record chemostratigraphically the boundary between the Pliensbachian and Toarcian and the higher levels of the latter stage (cf. Fig. 7). As illustrated by Jones *et al.* (1994) and in great detail by McArthur *et al.* (2000), in both cases based on more stratigraphically expanded sections from Yorkshire, the overall trend is for strontium-isotope ratios to fall through the Pliensbachian stage to reach a minimum value of ~0.707070 at the top of the *spinatum*/base of the *tenuicostatum* zone, a ratio that is regionally applicable across Europe, before rising through the whole of the following Toarcian stage to increasingly radiogenic values (cf. McArthur *et al.* 2019).

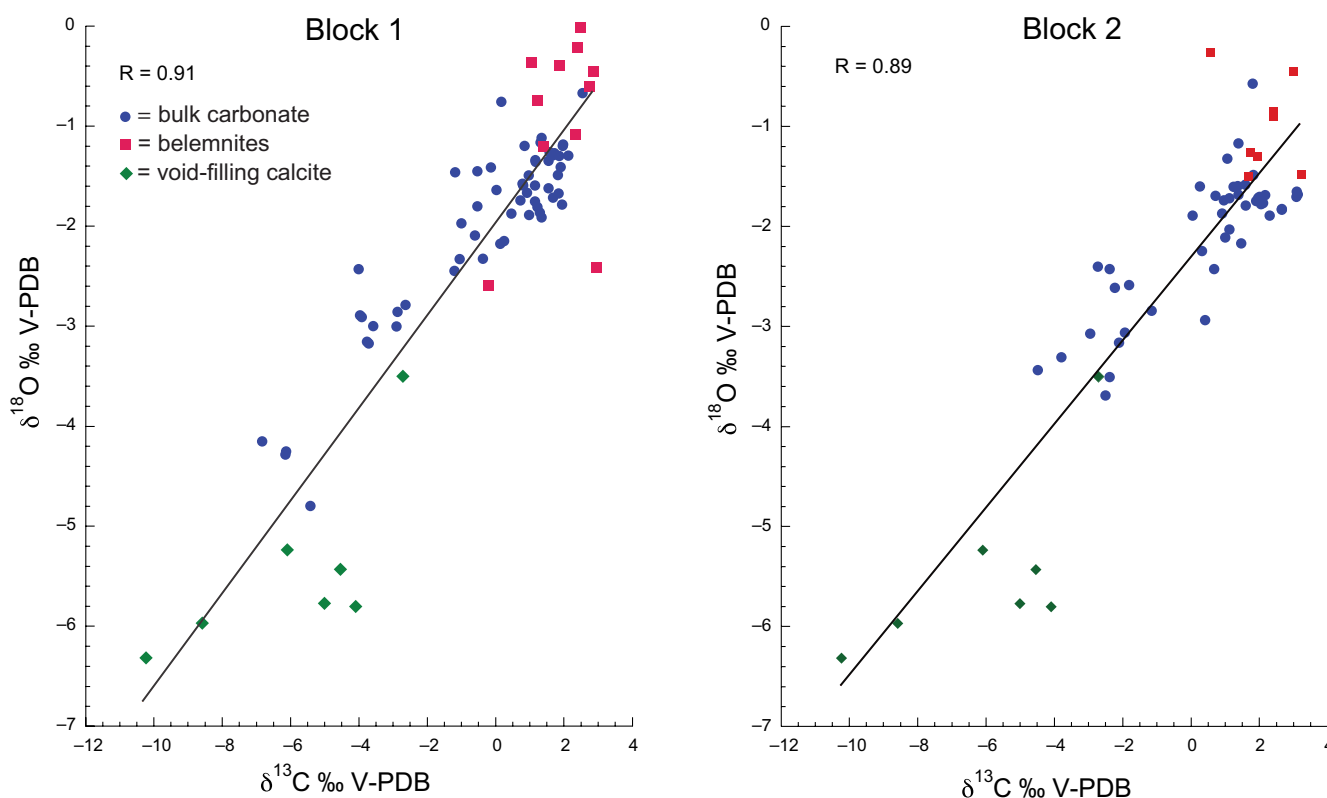


Fig. 8. (Colour online) Cross-plot of carbon and oxygen isotopes of bulk carbonate and belemnites from Blocks 1 and 2 and of diagenetic void-filling calcite from fissure facies sampled close to the Eype's Mouth Fault. The high values of the correlation coefficient in both plots is compatible with the matrix of the Marlstone and Junction Bed being formed primarily from a mixture of biological carbonate and diagenetic cement, the latter probably formed both on the sea floor and in the burial environment. Solid circles are bulk carbonate; solid squares are belemnites; solid diamonds are samples of diagenetic void-filling calcite from neptunian sills from close to the Eype's Mouth Fault.

An even lower figure (0.707003) is recorded from near the top of the Marlstone in Block 1 (Fig. 5), which must derive from an altered fossil given that this ratio is less than any Lower Jurassic value known from Europe (Fig. 7). Parenthetically, it may be noted that a diagenetic shift to lower than seawater values in belemnite calcite has been reported from Canada and New Zealand, where the interaction of the skeletal material with hydrothermal fluids has been postulated (Gröcke *et al.* 2007; Ullmann *et al.* 2013a). By contrast, the stratigraphically next highest belemnite on Block 1 has a value of 0.707198 (at 15–15.5 cm) that, at face value, places it around the *serpentinum*–*bifrons* zone boundary by comparison to reference curves. However, this seems unlikely to be a case of a stratigraphically adrift fossil (or matrix) and more probably the skeletal calcite has also been diagenetically modified somewhat, in this case to more radiogenic values, as the overlying three belemnites give relatively consistent values securely in the *serpentinum* zone. The succeeding next three belemnites, being the highest in the block, suggest the presence of the *bifrons* zone, possibly extending into the *variabilis* zone (Fig. 5).

The strontium-isotope pattern in Block 2 (Fig. 6) shows the same general pattern as in Block 1, with relatively low values (but no obvious trend) in the basal four belemnites in the Marlstone, compatible with a late Pliensbachian age, followed in the Junction Bed by a relatively abrupt rise to more radiogenic values typical of the Toarcian (Fig. 7). The two stratigraphically highest belemnites show values of 0.707188 and 0.707158, suggesting that the *serpentinum* zone possibly extends to this level. Accepted at face value, this is incompatible with a ratio of 0.707218, the highest recorded value in the section, in the underlying

belemnite (at the 20 cm level) that would place it in the *bifrons* zone. Either some diagenetic increase in strontium-isotope ratios is the case for this belemnite and/or the two stratigraphically highest belemnites have been differentially reworked from a stratigraphically lower level, which could explain the up-section fall in values as opposed to the expected rise (cf. McArthur *et al.* 2000). Notably, the belemnite analysed in the section at the 20 cm level is unusual in containing relatively elevated Fe and Mn contents, and is consequently probably altered and not reliable as a chemostratigraphic marker. Hence, most of the Junction Bed sampled in Block 2, which is thinner and probably less stratigraphically extensive than Block 1, probably pertains to the *serpentinum* zone, although the presence of higher zones at the top of the section is well possible, as tentatively indicated in Figure 6.

Overall, the strontium-isotope pattern in the lower Toarcian is most simply interpreted as recording a relative increase in the impact of global continental weathering and consequent fluvial input to the oceans as a major source of strontium, thereby outcompeting its input from basalt–seawater interaction such as submarine volcanism and/or sea-floor spreading (Jenkyns, 2003, 2010; Ullmann *et al.* 2013b).

4.b. Diagenesis

Examination of the carbon- and oxygen-isotope stratigraphic profiles of both Block 1 and Block 2 shows a high degree of parallelism, being particularly striking in the case of the negative excursions, of which there are several (Figs 5, 6). Such relationships are well illustrated in cross-plots (Fig. 8), in which additional

end-member data are supplied from the belemnites constituting primary skeletal material and also diagenetic void-filling sparry calcite from the fissure facies of the Junction Bed/Marlstone complex sampled adjacent to the Eype's Mouth Fault (Jenkyns & Senior, 1991). In Block 1, carbon-isotope values of most belemnites fall between 2 ‰ and 3 ‰ and most oxygen-isotope values between -2.5 ‰ and -0.4 ‰; in Block 2, carbon-isotope values of most belemnites fall between 1.7 ‰ and 3.0 ‰ and most oxygen-isotope values between -1.4 ‰ and -0.4 ‰. Carbon-isotope values of the void-filling calcite range between -2.71 ‰ and -10.23 ‰ with oxygen-isotope values ranging between -3.5 ‰ and -6.3 ‰. Given that the bulk carbonate isotopes of the Marlstone and Junction Bed lie in an intermediate position in terms of values, the data in the cross-plot can be interpreted as a two-component mixing 'line' representing different relative amounts of primary carbonate of biological origin and later diagenetic cements (cf. Marshall, 1992).

At least some of this diagenetic cement probably formed at or just below the sea floor, as indicated by the relative consolidation of the Marlstone/Junction Bed matrix injected by the neptunian sills next to the Eype's Mouth Fault. Additional evidence was cited by Jackson (1922) and Arkell (1933), who noted that vertically or sub-vertically planed-off ammonites in the Junction Bed, whose lower parts were held in micritic matrix, implied consolidation before syn-sedimentary erosion took place. Indeed, the overall slow net depositional rates of the Junction Bed would have been one of the prerequisites for open-marine submarine lithification (e.g., Milliman, 1966; Fischer & Garrison, 1967). However, the relatively negative carbon- and oxygen-isotope values of the fissure-fill calcitic cements, typically ferroan, suggest a subsequent late-stage component, probably derived from fluids formed by compacting and dewatering of underlying organic-rich shales and transferred along the conduit of the Eype's Mouth Fault (Raven & Dickson, 1989; Jenkyns & Senior, 1991). The relative importance of these possible processes as regards the lithification of the Junction Bed in normal facies, well separated from any fault is, however, not established. Notably, at Preston Plunknett (near Yeovil, Somerset), the carbon-isotope values of the *serpentinum* zone in the Junction Bed are ~1 ‰ heavier than those recorded in Blocks 1 and 2 and described herein (cf. Jenkyns & Clayton, 1997), suggesting a more minor role for late-stage diagenesis in at least some sections inland.

By contrast, the bulk carbon-isotope values in Toarcian coccolith-bearing pelagic red limestones from the Tethyan Jurassic of southern Europe (Italy, Greece) locally attain values of up to 4.5 ‰ in the *serpentinum* zone, and coeval belemnites from the organic-rich Jet Rock in Yorkshire attain values that exceed 6 ‰ in the upper *exaratum* subzone (Jenkyns & Clayton, 1986, 1997; Jenkyns *et al.* 2002; Sabatino *et al.* 2009; Kafousia *et al.* 2014). These figures are considerably in excess of the 1–2 ‰ background values of the Junction Bed exposed on the Dorset coast, equally suggesting possession of a considerable diagenetic overprint. The unusually high values in the Yorkshire belemnites, however, may relate to their having lived in somewhat isolated stratified basins where deposition of organic matter resulted in unusually elevated carbon-isotope values of local water-masses not characteristic of the open ocean (McArthur *et al.* 2008; Dickson *et al.* 2017; Remirez & Algeo, 2020).

4.c. The Toarcian Oceanic Anoxic Event

Recognition of the signature of the early Toarcian Oceanic Anoxic Event (T-OAE) in any lithological sequence relies, in the first

instance, on its exact definition. Using a combination of enhanced enrichment in organic carbon in globally distributed outcrops, and the accompanying carbonate and organic-matter carbon-isotope signature from a number of localities, suggests a duration from the mid-*tenuicostatum* zone (over which interval carbon-isotope values are generally rising) to the mid-*serpentinum* zone where values are typically at their highest, thereby taking in the intervening pronounced stepped negative carbon-isotope excursion that characterizes the T-OAE and interrupts the overarching positive trend (e.g. Jenkyns & Clayton, 1997; Hesselbo *et al.* 2000; Hermoso *et al.* 2009; Jenkyns, 2010; Kemp *et al.* 2011; Xu *et al.* 2018; Storm *et al.* 2020 for UK sequences). In northern and southern European outcrops, the most organic-rich level, typically developed as millimetre-laminated black shale, lies primarily in the lower part of the *exaratum* subzone of the *serpentinum* zone or its stratigraphic equivalents (Jenkyns *et al.* 2002).

The Junction Bed, with its prevailing red, pink, brown and yellow colours, suggests oxic conditions prevailed from the time of deposition into the burial environment: evidence that could be taken to indicate that no organic-rich sediment was ever deposited in this part of the Wessex Basin. It is, of course, possible that the particular palaeogeographic position of the Marlstone and Junction Bed in coastal Dorset, on a relatively non-subsiding sector of a tilted fault-block, was critical in this regard. In such a case, the sea floor, being possibly somewhat shallower than surrounding areas, may have remained persistently current-swept and oxic even if fluxes of organic matter through the water column were relatively elevated at the time.

However, the apparent absence of the lower *exaratum* subzone in the Junction Bed (Howarth, 1992) indicates that the key interval is likely represented by a hiatus, compatible with an interpretation that organic-rich sediment was initially deposited but was subsequently removed by sea-floor erosion. A little to the east (~40 km) of the outcrops on the Dorset coast, a somewhat more expanded section of the Junction Bed was encountered in the Winterborne Kingston Borehole where the T-OAE level is represented by shaly sediments containing up to 4% total organic carbon (Jenkyns & Clayton, 1997). Data from other wells in the region, including those in the offshore English Channel, include descriptions of lowermost Toarcian dark-coloured organic-rich 'paper shales' stratigraphically adjacent to the Junction Bed (Ainsworth *et al.* 1998; Ainsworth & Riley, 2010). Together, these records indicate that the major palaeoceanographic phenomenon represented by the T-OAE impacted the waters of the Wessex Basin, although the lack of its characteristic sedimentary signature in the Junction Bed of the Dorset coast cannot be ascribed unambiguously to any particular process.

Given that a pronounced negative carbon-isotope excursion, typically interrupting an overarching positive trend, is a feature of the T-OAE worldwide and recorded in pelagic and shallow-water carbonate, marine and terrestrial organic matter (e.g. Jenkyns & Clayton, 1997; Kemp *et al.* 2005; Hesselbo *et al.* 2007; Woodfine *et al.* 2008; Hermoso *et al.* 2009; Al-Suwaidi *et al.* 2010; Caruthers *et al.* 2011; Sabatino *et al.* 2013; Kemp & Izumi, 2014; Bodin *et al.* 2016; da Rocha *et al.* 2016; Them *et al.* 2017; Xu *et al.* 2017, 2018; Han *et al.* 2018; Ikeda *et al.* 2018; Kemp *et al.* 2020), it is possible that this signal is recorded in the Junction Bed. Where well dated, the core of the negative excursion lies in the basal *exaratum* subzone or equivalent (basal *serpentinum* zone), which is the interval that appears to be unrecorded in the Junction Bed and is likely lost to a hiatus (Howarth, 1992). It is, however, possible that some elements of the negative

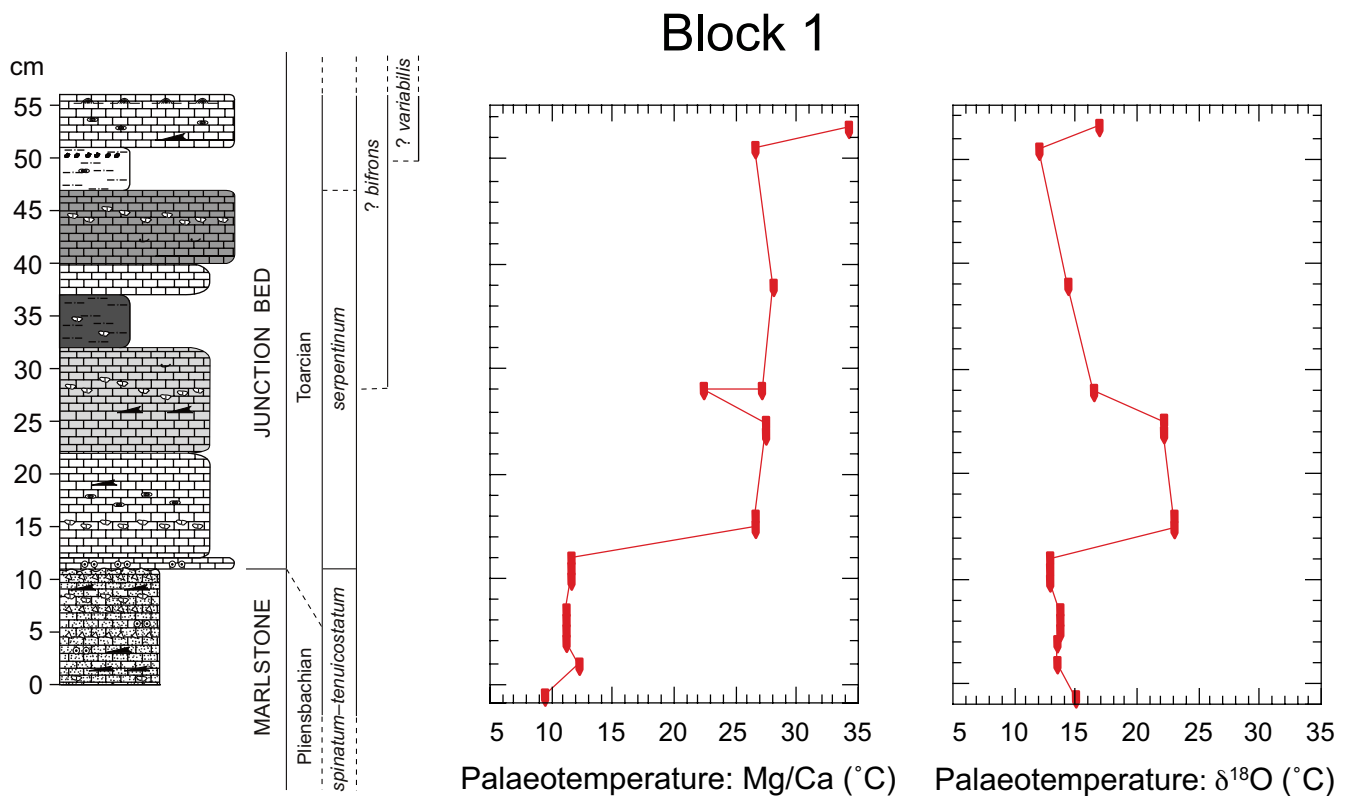


Fig. 9. (Colour online) Palaeotemperature reconstructions from oxygen-isotope values and Mg:Ca ratios from belemnites in Block 1. Oxygen-isotope-derived palaeotemperatures calculated using the formula of Anderson & Arthur (1983) applying a value of -1‰ SMOW for Mesozoic seawater; palaeotemperatures from Mg:Ca ratios in belemnites derived using the bivalve-based equation of Klein *et al.* (1996). Ammonite zones in italics.

carbon-isotope excursion (e.g. a rising and/or falling limb) are recorded in the Junction Bed and the pronounced shift at the 30–35 cm in Block 1 would be a possible candidate, given its likely position somewhere in the *serpentinum* zone, although this appears to be rather too high in the stratigraphy and could equally well be a diagenetic artefact. Of the negative excursions displayed in Block 2, all of which could also be entirely diagenetic in origin, that centred close to the boundary between the Marlstone and Junction Bed, probably extending into the basal *serpentinum* zone, is perhaps most likely to be a partial record of the T-OAE negative excursion. Correlation with lowered oxygen-isotope values and increased Mg:Ca ratios (Figs 5, 6) in this case could signify increased palaeotemperatures known to characterize this interval, as discussed below.

The general relatively low values of carbon isotopes in the underlying Marlstone seen in Blocks 1 and 2 (Figs 5, 6) could possibly be recording the negative excursion recently recognized in the *spinatum* zone (Storm *et al.* 2020), although the parallel shift in oxygen isotopes is equally compatible with a diagenetic interpretation. Other potential relatively minor carbon-isotope disturbances, such as those recorded from around the Pliensbachian–Toarcian boundary (Littler *et al.* 2010), cannot be positively identified in either block.

4.d. Palaeotemperatures: the Toarcian hyperthermal

The oxygen-isotope and Mg:Ca records of the belemnites potentially contain climatic information and point to a major increase in palaeotemperature across the Pliensbachian–Toarcian boundary or a little later. The signal is clearest in Block 1 (Fig. 5), which

illustrates a dramatic drop in oxygen-isotope values of $\sim 2.4\text{‰}$ with an accompanying jump in Mg:Ca ratios of ~ 10 mmol/mol in the lower *serpentinum* zone. The oxygen-isotope record, following the palaeotemperature equation of Anderson & Arthur (1983), translates into a rise of $\sim 10\text{ °C}$ from a background of $\sim 14\text{ °C}$ (Fig. 9). The incorporation of Mg into skeletal calcite is both temperature- and taxon-dependent and is hence unknown for extinct organisms such as belemnites, but application of the analysis of Bailey *et al.* (2003), who studied a large collection of these fossils from Yorkshire and Germany for Mg:Ca and oxygen-isotope ratios and found similar values to those given here, suggested that a temperature rise of 10–11 °C was plausible for the Wessex Basin. Recourse to the bivalve-derived Mg:Ca palaeotemperature equation of Klein *et al.* (1996) as applied to the belemnite data, given that both organisms belong to the same phylum, suggests a slightly greater rise ($\sim 15\text{ °C}$) from a background of $\sim 12\text{ °C}$ for Block 1 (Fig. 9). Higher in the section in Block 1, the signals diverge, with oxygen isotopes showing a general rise in values, potentially indicating cooler temperatures, whereas Mg:Ca ratios remain relatively high. The stratigraphically highest belemnite, if the proxy data are accepted at face value, suggests another increase in temperature in the *bifrons* zone or stratigraphically above, with the higher values indicated by the Mg:Ca ratios (Fig. 9).

The Mg:Ca pattern in Block 2 (Fig. 6) is rather similar to Block 1, although the oxygen-isotope shift is less pronounced. The increase in Mg:Ca ratios in the basal Toarcian is ~ 10 mmol/mol; the fall in oxygen-isotope ratios is $\sim 1\text{‰}$. Taken at face value, these figures suggests a more modest rise in temperature than do the data from Block 1 (Fig. 10), but are most likely a manifestation of the innate variability of the two proxies in question, particularly as

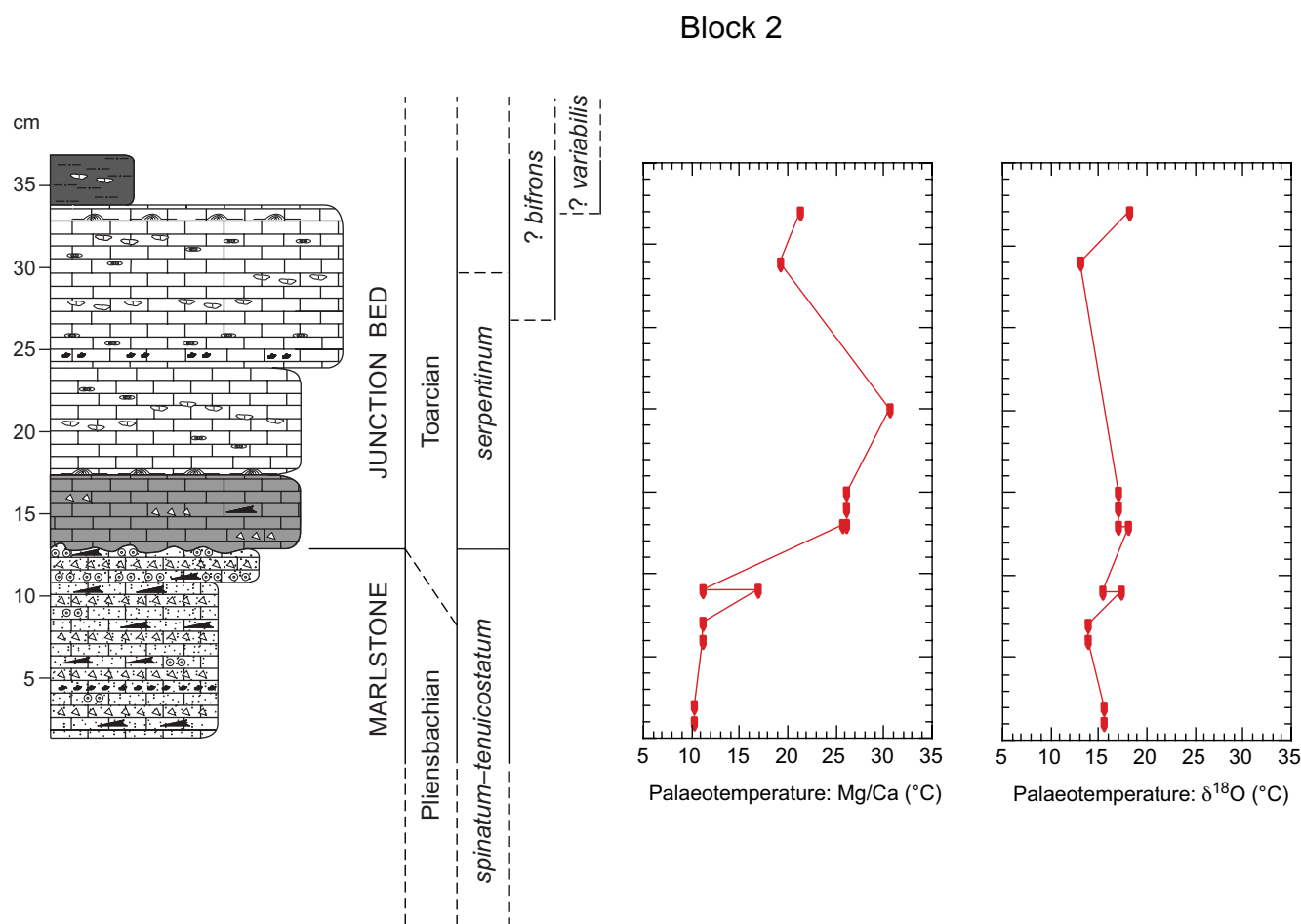


Fig. 10. (Colour online) Palaeotemperature reconstructions from oxygen-isotope values and Mg:Ca ratios from belemnites in Block 2. Oxygen-isotope-derived palaeotemperatures calculated using the formula of Anderson & Arthur (1983) applying a value of -1‰ smow for Mesozoic seawater; palaeotemperatures from Mg:Ca ratios in belemnites derived using the bivalve-based equation of Klein *et al.* (1996). Ammonite zones in italics.

changes in salinity operating on a variety of time scales could have been associated with both of them (Bailey *et al.* 2003; Rosales *et al.* 2004b; Ferguson *et al.* 2008).

Other potentially confounding factors implicated as controls on Mg:Ca ratios in belemnites include species-specific differences in the molluscs themselves, metabolic effects on trace-element incorporation, growth rates and diagenesis (McArthur *et al.* 2007; Li *et al.* 2012; Immenhauser *et al.* 2016; Ullmann & Pogge von Strandmann, 2017). The effects of diagenesis are most obviously seen in the belemnite from the 20 cm level in Block 2, whose Fe and Mn contents are also relatively elevated and whose strontium-isotope values appear anomalous (Fig. 6).

There is no doubt, however, that the vast range of data from palynology, particularly from the former Soviet Union, oxygen-isotope data from skeletal calcite (European belemnites and brachiopods), locally elevated levels of kaolinite in clay-mineral assemblages in north European sections, as well as novel TEX_{86} data (a rise of $\sim 10\text{ }^{\circ}\text{C}$ from a background of $\sim 22\text{ }^{\circ}\text{C}$, based on sections in Italy and Spain) and novel clumped isotope measurements (with a model increase of $13 \pm 4\text{ }^{\circ}\text{C}$ from the *spinatum* to *serpentinum* zones in belemnites from SW Germany), points to considerable warmth being a feature of the early Toarcian climate, thereby qualifying it as one of the major Mesozoic hyperthermals, as well as recording increased continental weathering, an oceanic anoxic event and an episode of ocean acidification (e.g. Vakhrameyev,

1982; Jenkyns & Clayton, 1997; McArthur *et al.* 2000; Jenkyns, 2003, 2010; Rosales *et al.* 2004a; Suan *et al.* 2010, 2011; Gomez & Goy, 2011; Dera *et al.* 2011a; Hermoso *et al.* 2012; Hönisch *et al.* 2012; Trecalli *et al.* 2012; Harazim *et al.* 2013; Hermoso & Pellenard, 2014; Fantasia *et al.* 2018; Müller *et al.* 2020; Ruebsam *et al.* 2020; Ullmann *et al.* 2020; Ettinger *et al.* 2021; Fernandez *et al.* 2021). Warming may have been primarily responsible for the northward spread of Mediterranean ammonites during the *tenuicostatum* and *serpentinum* zones (e.g. Dera *et al.* 2011b), also reflected by the presence of Tethyan gastropods and brachiopods in the Marlstone.

The coincident dramatic shift in oxygen isotopes, Mg:Ca ratios and $^{87}\text{Sr}/^{86}\text{Sr}$ values, most clearly seen in Block 1 and somewhat less obviously in Block 2 (Figs 5, 6), albeit likely being a function of condensation in the Marlstone and Junction Bed, is compatible with the view that the onset of hyperthermal conditions fostered an acceleration in continental weathering, thereby increasing the flux of radiogenic strontium to the oceans (Jenkyns, 2003, 2010; Ullmann *et al.* 2013b). The initial warming itself is conventionally attributed to supply of carbon dioxide during eruption of the Karoo–Ferrar Large Igneous Province, an interpretation supported by the presence, in a number of sections, of mercury assumed to be of volcanic and/or thermogenic origin and transmitted through the atmosphere to be ultimately fixed in organic-rich sediments (Pálffy & Smith, 2000; Svensen *et al.* 2007; Percival *et al.* 2015,

2016). Temperature-dependent dissociation of gas hydrates and/or metamorphism of organic-rich material, processes that would supply isotopically light carbon to the ocean–atmosphere system, have both been invoked as a prime cause of the negative carbon-isotope excursion that is one of the hallmarks of the T-OAE (Hesselbo *et al.* 2000; McElwain *et al.* 2005).

Finally, it should be noted that belemnites are thought to have been nektonic and likely record watermass characteristics below the thermocline that might have been ~14 °C cooler than sea-surface temperatures, based on comparative oxygen-isotope and TEX₈₆ data from Jurassic and Cretaceous sediments and their contained skeletal fossils (Mutterlose *et al.* 2010; Jenkyns *et al.* 2012). An exception to this rule may have been during the T-OAE when regionally developed expanded anoxic/euxinic bottom waters may have driven belemnites to occupy warmer nearer surface levels of the ocean (Ullmann *et al.* 2014).

5. Conclusions

The stratigraphically condensed Marlstone and overlying Junction Bed (Pliensbachian–Toarcian) in coastal Dorset, UK (Wessex Basin) have yielded a range of chemostratigraphic data: ⁸⁷Sr/⁸⁶Sr, δ¹³C, δ¹⁸O and Mg:Ca of belemnites and δ¹³C and δ¹⁸O of bulk carbonate. Although the fossil-rich matrix of the Marlstone and Junction Bed shows a significant diagenetic overprint, the isotopic signals from the contained belemnites reflect global trends, such as increasing radiogenic ⁸⁷Sr/⁸⁶Sr values from a relative minimum around the Pliensbachian–Toarcian boundary, at which level there is evidence for a dramatic rise in temperature illustrated by δ¹⁸O and Mg:Ca of the fossil skeletal calcite. With regard to the T-OAE, there is no trace of organic-rich sediment anywhere in the Junction Bed, which could be due in part to the apparent absence of the lower *exaratum* subzone in the unit, which elsewhere in the UK is developed as laminated black shale. Alternatively, oxic conditions may have prevailed on the sea floor throughout the deposition of the Junction Bed. Possible signatures of the negative δ¹³C excursion that accompanies the T-OAE in sequences worldwide are present in the bulk carbon-isotope curve in the putative *serpentinum* zone, although they could also be interpreted as diagenetic artefacts. With its striking pink, yellow, red and brown colours, stromatolitic layers and enrichment in Fe–Mn oxyhydroxides, the Junction Bed and to a lesser extent the Marlstone recall certain highly condensed pelagic facies of the Tethyan Jurassic such as the Rosso Ammonitico and a similar depositional context is likely, namely on the relatively non-subsident sector of a complex half-graben system.

Supplementary material. To view supplementary material for this article, please visit <https://doi.org/10.1017/S0016756821000972>

Acknowledgements. Thanks are due to John Arden, Julie Cartledge, Stephen Hesselbo, Stuart Robinson, Richard Woodfine, Steve Wyatt and two anonymous referees for their help with this paper. The study was supported by the Department of Earth Sciences, University of Oxford. Numerical data are given in the online Supplementary Material.

References

- Ager DV (1956) The geographical distribution of brachiopods in the British Middle Lias. *Quarterly Journal of the Geological Society of London* **112**, 157–87.
- Ainsworth NR, Braham W, Gregory FJ, Johnson B and King C (1998) The lithostratigraphy of the latest Triassic to earliest Cretaceous of the English Channel and its adjacent areas. In *Development, Evolution and Petroleum Geology of the Wessex Basin* (ed. JR Underhill), pp. 103–64. Geological Society of London, Special Publication no. 133.
- Ainsworth NR and Riley LA (2010) Triassic to Middle Jurassic stratigraphy of the Kerr McGee 97/12-1 exploration well, offshore southern England. *Marine and Petroleum Geology* **27**, 853–84.
- Al-Suwaidi AH, Angelozzi GN, Damborenea SE, Hesselbo SP, Jenkyns HC, Manceñido MO and Riccardi AC (2010) First record of the Early Toarcian oceanic anoxic event from the Southern Hemisphere, Neuquén Basin, Argentina. *Journal of the Geological Society, London* **167**, 633–6.
- Anderson TF and Arthur MA (1983) Stable isotopes of oxygen and carbon and their application to sedimentologic and paleoenvironmental problems. In *Stable Isotopes in Sedimentary Geology* (contributors MA Arthur, TF Anderson, IR Kaplan, J Veizer and LS Land), pp. 1–151. Society of Economic Paleontologists and Mineralogists Short Course No. 10.
- Arkell WJ (1933) *The Jurassic System in Great Britain*. London: Oxford University Press, 681 pp.
- Bailey TR, Rosenthal Y, McArthur JM, van de Schootbrugge B and Thirlwall MF (2003) Paleooceanographic changes of the Late Pliensbachian–Early Toarcian interval: a possible link to the genesis of an Oceanic Anoxic Event. *Earth and Planetary Science Letters* **212**, 307–20.
- Bernoulli D and Jenkyns HC (1974) Alpine, Mediterranean and central Atlantic Mesozoic facies in relation to the early evolution of the Tethys. In *Modern and Ancient Geosynclinal Sedimentation* (eds RH Dott Jr and RH Shaver), pp. 129–60. Society of Economic Paleontologists and Mineralogists Special Publication 19.
- Bodin S, Krencker FN, Kothe T, Hoffmann R, Mattioli E, Heimhofer U and Kabiri L (2016) Perturbation of the carbon cycle during the late Pliensbachian–early Toarcian: new insight from high-resolution carbon isotope records in Morocco. *Journal of African Earth Sciences* **116**, 89–104.
- Boomer I, Copestake P, Page K, Huxtable J, Loy T, Bown P, Jones TD, O’Callaghan M, Hawkes S, Halfacree D and Reay H (2021) Biotic and stable-isotope characterization of the Toarcian Ocean Anoxic Event through a carbonate–clastic sequence from Somerset, UK. In *Carbon Cycle and Ecosystem Response to the Jenkyns Event in the Early Toarcian (Jurassic)* (eds M Reolid, LV Duarte, E Mattioli and W Ruebsam). Geological Society of London, Special Publication no. 514, published online 5 July 2021. doi: [10.1144/SP514-2020-263](https://doi.org/10.1144/SP514-2020-263).
- Boomer I, Lord AR, Page KN, Bown PR, Lowry FMD and Riding JB (2009) The biostratigraphy of the Upper Pliensbachian–Toarcian (Lower Jurassic) sequence at Ilminster, Somerset. *Journal of Micropalaeontology* **28**, 67–85.
- Buckman SS (1922) Jurassic chronology: II—preliminary studies. Certain Jurassic strata near Eynesmouth (Dorset); the Junction-Bed of Wotton Cliff and associated rocks. *Quarterly Journal of the Geological Society of London* **78**, 378–457.
- Caruthers AH, Gröcke DR and Smith PL (2011) The significance of an Early Jurassic (Toarcian) carbon-isotope excursion in Haida Gwaii (Queen Charlotte Islands), British Columbia, Canada. *Earth and Planetary Science Letters* **307**, 19–26.
- Chadwick RA (1986) Extension tectonics in the Wessex Basin, southern England. *Journal of the Geological Society, London* **143**, 465–88.
- Conti MA and Monari S (2003) Jurassic dischelicid gastropods from the Reatini Mountains (central Apennines, Italy) and their stratigraphical significance. *Geologica Romana* **36**, 199–213.
- Cope JCW, Getty TA, Howarth MK, Morton N and Torrens HS (1980) *A Correlation of Jurassic Rocks in the British Isles; Part One: Introduction and Lower Jurassic*. Geological Society of London, Special Report No. 14, 73 pp.
- Cox BM, Sumner MG and Ivimey-Cook HC (1999) A formational framework for the Lower Jurassic of England and Wales (Onshore Area). British Geological Survey Research Report RR/99/01, 25 pp.
- Cronan DS, Galác A, Mindszenty A, Moorby SA and Polgari M (1991) Tethyan ferromanganese oxide deposits from Jurassic rocks in Hungary. *Journal of the Geological Society, London* **148**, 655–68.
- da Rocha RB, Mattioli E, Duarte L, Pittet B, Elmi S, Mouterde R, Cabral MC, Comas-Rengifo M, Gómez J, Goy A, Hesselbo S, Jenkyns HC, Littler K, Mailliot S, de Oliveira LCV, Osete ML, Perilli N, Pinto S, Ruget C and

- Suan G (2016) Base of the Toarcian Stage of the Lower Jurassic defined by the Global Boundary Stratotype Section and Point (GSSP) at the Peniche section (Portugal). *Episodes* **39**, 460–81.
- Dera G, Brigaud B, Monna F, Laffont R, Puc at E, Deconinck J-F, Pellenard P, Joachimski MM and Durllet C (2011a) Climatic ups and downs in a disturbed Jurassic world. *Geology* **39**, 215–18.
- Dera G, Neige P, Dommergues JL and Brayard A (2011b) Ammonite paleobiogeography during the Pliensbachian–Toarcian crisis (Early Jurassic) reflecting paleoclimate, eustasy, and extinctions. *Global and Planetary Change* **78**, 92–105.
- Dickson AJ, Gill BC, Ruhl M, Jenkyns HC, Porcelli D, Idiz E, Lyons TW and van den Boorn SH (2017) Molybdenum-isotope chemostratigraphy and paleoceanography of the Toarcian Oceanic Anoxic Event (Early Jurassic). *Paleoceanography* **328**, 13–829.
- Ettlinger NP, Larson TE, Kerans C, Thibodeau AM, Hattori KE, Kacur SM and Martindale RC (2021) Ocean acidification and photic-zone anoxia at the Toarcian Oceanic Anoxic Event: insights from the Adriatic Carbonate Platform. *Sedimentology* **68**, 63–107.
- Fantasia A, F ollmi KB, Adatte T, Spangenberg JE and Montero-Serrano JC (2018) The Early Toarcian oceanic anoxic event: paleoenvironmental and paleoclimatic change across the Alpine Tethys (Switzerland). *Global and Planetary Change* **162**, 53–68.
- Ferguson JE, Henderson GM, Kucera M and Rickaby REM (2008) Systematic change of foraminiferal Mg/Ca ratios across a strong salinity gradient. *Earth and Planetary Science Letters* **265**, 153–66.
- Fernandez A, Korte C, Ullmann CV, Looser N, Wohlwend S and Bernasconi SM (2021) Reconstructing the magnitude of Early Toarcian (Jurassic) warming using the reordered clumped isotope compositions of belemnites. *Geochimica et Cosmochimica Acta* **293**, 308–27.
- Fischer AG and Garrison RE (1967) Carbonate lithification on the sea floor. *Journal of Geology* **75**, 488–96.
- F ollmi KB (2016) Sedimentary condensation. *Earth-Science Reviews* **152**, 143–80.
- G omez JJ and Goy A (2011) Warming-driven mass extinction in the Early Toarcian (Early Jurassic) of northern and central Spain. Correlation with other time-equivalent European sections. *Palaeogeography, Palaeoclimatology, Palaeoecology* **306**, 176–95.
- Gr ocke D, Hesselbo SP and Findlay DJ (2007) Atypical diagenetic effects on strontium-isotope composition of Early Jurassic belemnites, Queen Charlotte Islands, British Columbia, Canada. *Canadian Journal of Earth Sciences* **44**, 181–97.
- Hallam A (1967) A sedimentary and faunal study of the Blue Lias of Dorset and Glamorgan. *Philosophical Transactions of the Royal Society, Series B* **243**, 1–44.
- Han Z, Hu X, Kemp DB and Li J (2018) Carbonate-platform response to the Toarcian Oceanic Anoxic Event in the southern hemisphere: implications for climatic change and biotic platform demise. *Earth and Planetary Science Letters* **489**, 59–71.
- Harazim D, van de Schootbrugge B, Sorichter K, Fiebig J, Weug A, Suan G and Oschmann W (2013) Spatial variability of watermass conditions within the European Epicontinental Seaway during the Early Jurassic (Pliensbachian–Toarcian). *Sedimentology* **60**, 359–90.
- Hermoso M, Le Callonnec L, Minoletti F, Renard M and Hesselbo SP (2009) Expression of the Early Toarcian negative carbon-isotope excursion in separated carbonate microfractions (Jurassic, Paris Basin). *Earth and Planetary Science Letters* **277**, 194–203.
- Hermoso M, Minoletti F, Rickaby RE, Hesselbo SP, Baudin F and Jenkyns HC (2012) Dynamics of a stepped carbon-isotope excursion: ultra high-resolution study of Early Toarcian environmental change. *Earth and Planetary Science Letters* **319**, 45–54.
- Hermoso M and Pellenard P (2014) Continental weathering and climatic changes inferred from clay mineralogy and paired carbon isotopes across the early to middle Toarcian in the Paris Basin. *Palaeogeography, Palaeoclimatology, Palaeoecology* **399**, 385–93.
- Hesselbo SP, Gr ocke DR, Jenkyns HC, Bjerrum CJ, Farrimond P, Morgans Bell HS and Green OR (2000) Massive dissociation of gas hydrate during a Jurassic oceanic anoxic event. *Nature* **406**, 392–5.
- Hesselbo SP and Jenkyns HC (1995) A comparison of the Hettangian to Bajocian successions of Dorset and Yorkshire. In *Field Geology of the British Jurassic* (ed. PD Taylor), pp. 105–50. London: Geological Society of London.
- Hesselbo SP, Jenkyns HC, Duarte LV and Oliveira LC (2007) Carbon-isotope record of the Early Jurassic (Toarcian) Oceanic Anoxic Event from fossil wood and marine carbonate (Lusitanian Basin, Portugal). *Earth and Planetary Science Letters* **253**, 455–70.
- H onisch B, Ridgwell A, Schmidt DN, Thomas E, Gibbs SJ, Sluijs A, Zeebe R, Kump L, Martindale RC, Greene SE, Kiessling W, Ries J, Zachos JC, Royer DL, Barker S, Marchitto TM Jr, Moyer R, Pelejero C, Ziveri P, Foster GL and Williams BC (2012) The geological record of ocean acidification. *Science* **335**, 1058–63.
- Howarth MK (1957) The middle Lias of the Dorset coast. *Quarterly Journal of the Geological Society of London* **113**, 185–204.
- Howarth MK (1980) The Toarcian age of the upper part of the Marlstone Rock Bed of England. *Palaeontology* **23**, 637–56.
- Howarth MK (1992) The ammonite family Hildoceratidae in the Lower Jurassic of Britain. Part 1. *Monograph of the Palaeontographical Society London* **145** (Publ. No. 586), 1–106.
- Ikeda M, Hori RS, Ikehara M, Miyashita R, Chino M and Yamada K (2018) Carbon cycle dynamics linked with Karoo-Ferrar volcanism and astronomical cycles during Pliensbachian–Toarcian (Early Jurassic). *Global and Planetary Change* **170**, 163–71.
- Immenhauser A, Schoene BR, Hoffmann R and Niedermayr A (2016) Mollusc and brachiopod skeletal hard parts: intricate archives of their marine environment. *Sedimentology* **63**, 1–59.
- Jackson JF (1922) Sections of the Junction-Bed and contiguous deposits. *Quarterly Journal of the Geological Society of London* **78**, 436–48.
- Jackson JF (1926) The Junction-Bed of the Middle and Upper Lias on the Dorset Coast. *Quarterly Journal of the Geological Society of London* **82**, 490–525.
- Jenkyns HC (1970) Fossil manganese nodules from the west Sicilian Jurassic. *Elogae Geologicae Helveticae* **63**, 741–74.
- Jenkyns HC (1971) The genesis of condensed sequences in the Tethyan Jurassic. *Lethaia* **4**, 327–52.
- Jenkyns HC (2003) Evidence for rapid climate change in the Mesozoic–Palaeogene greenhouse world. *Philosophical Transactions of the Royal Society of London, Series A* **361**, 1885–916.
- Jenkyns HC (2010) Geochemistry of oceanic anoxic events. *Geochemistry, Geophysics, Geosystems* **11**, Q03004. doi: [10.1029/2009GC002788](https://doi.org/10.1029/2009GC002788)
- Jenkyns HC and Clayton CJ (1986) Black shales and carbon isotopes in pelagic sediments from the Tethyan Lower Jurassic. *Sedimentology* **33**, 87–106.
- Jenkyns HC and Clayton CJ (1997) Lower Jurassic epicontinental carbonates and mudstones from England and Wales: chemostratigraphic signals and the early Toarcian anoxic event. *Sedimentology* **44**, 687–706.
- Jenkyns HC, Jones CE, Gr ocke DR, Hesselbo SP and Parkinson DN (2002) Chemostratigraphy of the Jurassic System: applications, limitations and implications for palaeoceanography. *Journal of the Geological Society, London* **159**, 351–78.
- Jenkyns HC, Schouten-Huibers L, Schouten S and Sinninghe Damst e JS (2012) Warm Middle Jurassic–Early Cretaceous high-latitude sea-surface temperatures from the Southern Ocean. *Climate of the Past* **8**, 215–26.
- Jenkyns HC and Senior JR (1977) A Liassic palaeofault from Dorset. *Geological Magazine* **114**, 47–52.
- Jenkyns HC and Senior JR (1991) Geological evidence for intra-Jurassic faulting in the Wessex Basin and its margins. *Journal of the Geological Society, London* **148**, 245–60.
- Jenkyns HC and Torrens HS (1971) Palaeogeographic evolution of Jurassic seamounts in Western Sicily. In *Colloque du Jurassique m editerran een* (ed. E V egh-Neubrandt), pp. 91–104. Annales Instituti Geologici Publici Hungarici 54.
- Jones CE, Jenkyns HC and Hesselbo SP (1994) Strontium isotopes in Early Jurassic seawater. *Geochimica et Cosmochimica Acta* **58**, 1285–301.
- Kafousia N, Karakitsios V, Mattioli E, Kenjo S and Jenkyns HC (2014) The Toarcian Oceanic Anoxic Event in the Ionian Zone, Greece. *Palaeogeography, Palaeoclimatology, Palaeoecology* **393**, 135–45.

- Karner GD, Lake SD and Dewey JF (1987) The thermal and mechanical development of the Wessex Basin, southern England. In *Continental Extensional Tectonics* (eds MP Coward, JF Dewey and PL Hancock), pp. 517–36. Geological Society of London, Special Publication no. 28.
- Kemp DB, Coe AL, Cohen AS and Schwark L (2005) Astronomical pacing of methane release in the Early Jurassic period. *Nature* **437**, 396–9.
- Kemp DB, Coe AL, Cohen AS and Weedon GP (2011) Astronomical forcing and chronology of the early Toarcian (Early Jurassic) oceanic anoxic event in Yorkshire, UK. *Paleoceanography* **26**, PA4210. doi: [10.1029/2011PA002122](https://doi.org/10.1029/2011PA002122).
- Kemp DB and Izumi K (2014) Multiproxy geochemical analysis of a Panthalassic margin record of the early Toarcian oceanic anoxic event (Toyora area, Japan). *Palaeogeography, Palaeoclimatology, Palaeoecology* **414**, 332–41.
- Kemp DB, Selby D and Izumi K (2020) Direct coupling between carbon release and weathering during the Toarcian oceanic anoxic event. *Geology* **48**, 976–80.
- King A (2011) Fossil nautiloids from the Upper Lias (Toarcian) 'Junction Bed' of the Ilminster Area, Somerset. *Proceedings of the Somerset Archaeological and Natural History Society* **154**, 249–58.
- Klein RT, Lohmann KC and Thayer CW (1996) Bivalve skeletons record sea-surface temperature and $\delta^{18}\text{O}$ via Mg/Ca and $^{18}\text{O}/^{16}\text{O}$ ratios. *Geology* **24**, 415–18.
- Li Q, McArthur JM and Atkinson TC (2012) Lower Jurassic belemnites as indicators of palaeo-temperature. *Palaeogeography, Palaeoclimatology, Palaeoecology* **315–316**, 38–45.
- Littler K, Hesselbo SP and Jenkyns HC (2010) A carbon-isotope perturbation at the Pliensbachian–Toarcian boundary: evidence from the Lias Group, NE England. *Geological Magazine* **147**, 181–92.
- Marshall JD (1992) Climatic and oceanographic isotopic signals from the carbonate rock record and their preservation. *Geological Magazine* **129**, 143–60.
- Massari F and Westphal H (2011) Microbialites in the Middle–Upper Jurassic Ammonitico Rosso of the Southern Alps (Italy). In *Stromatolites: Interaction of Microbes with Sediments* (eds V Tewari and J Seckbach), pp. 223–50. Dordrecht: Springer.
- McArthur JM, Algeo TJ, van de Schootbrugge B, Li Q and Howarth RJ (2008) Basinal restriction, black shales, Re-Os dating, and the Early Toarcian (Jurassic) oceanic anoxic event. *Paleoceanography* **23**, PA4217. doi: [10.1029/2008PA001607](https://doi.org/10.1029/2008PA001607).
- McArthur JM, Donovan DT, Thirlwall MF, Fouke BW and Matthey D (2000) Strontium isotope profile of the early Toarcian (Jurassic) oceanic anoxic event, the duration of ammonite biozones, and belemnite palaeotemperatures. *Earth and Planetary Science Letters* **179**, 269–85.
- McArthur JM, Doyle P, Leng MJ, Reeves K, Williams CT, Garcia-Sanchez R and Howarth RJ (2007) Testing palaeo-environmental proxies in Jurassic belemnites: Mg/Ca, Sr/Ca, Na/Ca, $\delta^{18}\text{O}$ and $\delta^{13}\text{C}$. *Palaeogeography, Palaeoclimatology, Palaeoecology* **252**, 464–80.
- McArthur JM, Howarth RJ and Bailey TR (2001) Strontium isotope stratigraphy: LOWESS version 3: best fit to the marine Sr-isotope curve for 0–509 Ma and accompanying look-up table for deriving numerical age. *Journal of Geology* **109**, 155–70.
- McArthur JM, Page K, Duarte LV, Thirlwall MF, Li Q, Weis R and Comas-Rengifo MJ (2019) Sr-isotope stratigraphy ($^{87}\text{Sr}/^{86}\text{Sr}$) of the lowermost Toarcian of Peniche, Portugal, and its relation to ammonite zonation. *Newsletters on Stratigraphy* **53**, 297–32.
- McElwain JC, Wade-Murphy J and Hesselbo SP (2005) Changes in carbon dioxide during an oceanic anoxic event linked to intrusion into Gondwana coals. *Nature* **435**, 479–82.
- Milliman JD (1966) Submarine lithification of carbonate sediments. *Science* **153**, 994–7.
- Müller T, Jurikova H, Gutjahr M, Tomašových A, Schlögl J, Liebetrau V, Duarte LV, Milovský R, Mattioli E and Pittet B (2020) Ocean acidification during the early Toarcian extinction event: evidence from boron isotopes in brachiopods. *Geology* **48**, 1184–8.
- Mutterlose J, Malkoc M, Schouten S, Sinninghe Damsté JS and Forster A (2010) TEX_{86} and stable $\delta^{18}\text{O}$ paleothermometry of early Cretaceous sediments: implications for belemnite ecology and paleotemperature proxy application. *Earth and Planetary Science Letters* **298**, 286–98.
- Nieto LM, Ruiz-Ortiz PA, Rey J and Benito MI (2008) Strontium-isotope stratigraphy as a constraint on the age of condensed levels: examples from the Jurassic of the Subbetic Zone (southern Spain). *Sedimentology* **55**, 1–29.
- Pálffy J and Smith PL (2000) Synchrony between Early Jurassic extinction, oceanic anoxic event, and the Karoo–Ferrar flood basalt volcanism. *Geology* **28**, 747–50.
- Percival LME, Witt MLI, Mather TA, Hermoso M, Jenkyns HC, Hesselbo SP, Al-Suwaidi AH, Storm MS, Xu W and Ruhl M (2015) Globally enhanced mercury deposition during the end-Pliensbachian extinction and Toarcian OAE: a link to the Karoo–Ferrar Large Igneous Province. *Earth and Planetary Science Letters* **428**, 267–80.
- Percival LME, Cohen AS, Davies MK, Dickson AJ, Hesselbo SP, Jenkyns HC, Leng MJ, Mather TA, Storm MS and Xu W (2016) Osmium isotope evidence for two pulses of increased continental weathering linked to Early Jurassic volcanism and climate change. *Geology* **44**, 759–62.
- Prescott DM (1988) The geochemistry and palaeoenvironmental significance of iron pisoliths and ferromanganese crusts from the Jurassic of Mallorca, Spain. *Eclogae Geologicae Helvetiae* **81**, 387–414.
- Raven MJ and Dickson JAD (1989) Fir-tree zoning: an indicator of pulsed crystallization in calcite cement crystals. *Sedimentary Geology* **65**, 249–59.
- Remirez MN and Algeo TJ (2020) Carbon-cycle changes during the Toarcian (Early Jurassic) and implications for regional versus global drivers of the Toarcian oceanic anoxic event. *Earth-Science Reviews* **209**, 103283. doi: [10.1016/j.earscirev.2020.103283](https://doi.org/10.1016/j.earscirev.2020.103283).
- Reolid M (2011) Palaeoenvironmental contexts for microbial communities from Fe–Mn crusts of Middle–Upper Jurassic hardgrounds (Betic–Rifian Cordillera). *Revista Española de Paleontología* **26**, 135–60.
- Rosales I, Quesada S and Robles S (2004a) Paleotemperature variations of Early Jurassic seawater recorded in geochemical trends of belemnites from the Basque–Cantabrian basin, northern Spain. *Palaeogeography, Palaeoclimatology, Palaeoecology* **203**, 253–75.
- Rosales I, Robles S and Quesada S (2004b) Elemental and oxygen isotope composition of Early Jurassic belemnites: salinity vs. temperature signals. *Journal of Sedimentary Research* **74**, 342–54.
- Rosenthal Y, Boyle EA and Slowey N (1997) Temperature control on the incorporation of magnesium, strontium, fluorine, and cadmium into benthic foraminiferal shells from Little Bahama Bank: prospects for thermocline paleoceanography. *Geochimica et Cosmochimica Acta* **61**, 3633–43.
- Ruebsam W, Reolid M, Sabatino N, Masetti D and Schwark L (2020) Molecular paleothermometry of the early Toarcian climate perturbation. *Global and Planetary Change* **195**, 103351. doi: [10.1016/j.gloplacha.2020.103351](https://doi.org/10.1016/j.gloplacha.2020.103351).
- Sabatino N, Neri R, Bellanca A, Jenkyns HC, Baudin F, Parisi G and Masetti D (2009) Carbon-isotope records of the Early Jurassic (Toarcian) oceanic anoxic event from the Valdorbia (Umbria–Marche Apennines) and Monte Mangart (Julian Alps) sections: palaeoceanographic and stratigraphic implications. *Sedimentology* **56**, 1307–28.
- Sabatino N, Vlahović I, Jenkyns HC, Scopelliti G, Neri R, Prtoljan B and Velić I (2013) Carbon-isotope record and palaeoenvironmental changes during the early Toarcian oceanic anoxic event in shallow-marine carbonates of the Adriatic Carbonate Platform in Croatia. *Geological Magazine* **150**, 1085–102.
- Scopelliti G and Russo V (2021) Petrographic and geochemical characterization of the Middle–Upper Jurassic Fe–Mn crusts and mineralizations from Monte Inici (north-western Sicily): genetic implications. *International Journal of Earth Sciences* **110**, 559–82.
- Sellwood BW, Durkin MK and Kennedy WJ (1970) Field meeting on the Jurassic and Cretaceous rocks of Wessex. *Proceedings of the Geologists' Association* **81**, 715–32.
- Sellwood BW and Jenkyns HC (1975) Basins and swells and the evolution of an epeiric sea (Pliensbachian–Bajocian of Great Britain). *Journal of the Geological Society, London* **131**, 373–88.
- Storm MS, Hesselbo SP, Jenkyns HC, Ruhl M, Ullmann CV, Xu W, Leng MJ, Riding JB and Gorbanenko O (2020) Orbital pacing and secular evolution of the Early Jurassic carbon cycle. *Proceedings of the National Academy of Sciences* **117**, 3974–82.

- Suan G, Mattioli E, Pittet B, Lécuyer C, Suchéras-Marx B, Duarte LV, Philippe M, Reggiani L and Martineau F** (2010) Secular environmental precursors to Early Toarcian (Jurassic) extreme climate changes. *Earth and Planetary Science Letters* **290**, 448–58.
- Suan G, Nikitenko BL, Rogov MA, Baudin F, Spangenberg JE, Knyazev VG, Glinskikh LA, Goryacheva AA, Adatte T, Riding JB and Föllmi KB** (2011) Polar record of Early Jurassic massive carbon injection. *Earth and Planetary Science Letters* **312**, 102–13.
- Svensen H, Planke S, Chevillier L, Malthé-Sørenssen A, Corfu F and Jamtveit B** (2007) Hydrothermal venting of greenhouse gases triggering Early Jurassic global warming. *Earth and Planetary Science Letters* **256**, 554–66.
- Them II TR, Gill BC, Caruthers AH, Gröcke DR, Tulskey ET, Martindale RC, Poulton TP and Smith PL** (2017) High-resolution carbon isotope records of the Toarcian Oceanic Anoxic Event (Early Jurassic) from North America and implications for the global drivers of the Toarcian carbon cycle. *Earth and Planetary Science Letters* **459**, 118–26.
- Trecalli A, Spangenberg J, Adatte T, Föllmi KB and Parente M** (2012) Carbonate platform evidence of ocean acidification at the onset of the early Toarcian oceanic anoxic event. *Earth and Planetary Science Letters* **357**, 214–25.
- Ullmann CV, Boyle R, Duarte LV, Hesselbo SP, Kasemann SA, Klein T, Lenton TM, Piazza V and Aberhan M** (2020) Warm afterglow from the Toarcian Oceanic Anoxic Event drives the success of deep-adapted brachiopods. *Scientific Reports* **10**, 6549. doi: [10.1038/s41598-020-63487-6](https://doi.org/10.1038/s41598-020-63487-6).
- Ullmann CV, Campbell HJ, Frei R, Hesselbo SP, von Strandmann PAP and Korte C** (2013a) Partial diagenetic overprint of Late Jurassic belemnites from New Zealand: implications for the preservation potential of $\delta^7\text{Li}$ values in calcite fossils. *Geochimica et Cosmochimica Acta* **120**, 80–96.
- Ullmann CV, Hesselbo SP and Korte C** (2013b) Tectonic forcing of Early to Middle Jurassic seawater Sr/Ca. *Geology* **41**, 1211–14.
- Ullmann CV and Pogge von Strandmann PA** (2017) The effect of shell secretion rate on Mg/Ca and Sr/Ca ratios in biogenic calcite as observed in a belemnite rostrum. *Biogeosciences* **14**, 89–97.
- Ullmann CV, Thibault N, Ruhl M, Hesselbo SP and Korte C** (2014) Effect of a Jurassic oceanic anoxic event on belemnite ecology and evolution. *Proceedings of the National Academy of Sciences* **111**, 10073–6.
- Vakhrameyev VA** (1982) *Classopollis* pollen as an indicator of Jurassic and Cretaceous climate. *International Geology Review* **24**, 1190–6.
- Vera JA and Martín-Algarra A** (1994) Mesozoic stratigraphic breaks and pelagic stromatolites in the Betic Cordillera, Southern Spain. In *Phanerozoic Stromatolites II* (eds J Bertrand-Sarfati and C Monty), pp. 319–44. Dordrecht: Springer.
- Wendt J** (1968) *Discohelix* (Archaeogastropoda, Euomphalacea) as an index fossil in the Tethyan Jurassic. *Palaeontology* **11**, 554–75.
- Woodfine RG, Jenkyns HC, Sarti M, Baroncini F and Violante C** (2008) The response of two Tethyan carbonate platforms to the early Toarcian (Jurassic) oceanic anoxic event: environmental change and differential subsidence. *Sedimentology* **55**, 1011–28.
- Xu W, Ruhl M, Jenkyns HC, Hesselbo SP, Riding JB, Selby D, Naafs BDA, Weijers JW, Pancost RD, Tegelaar EW and Idiz EF** (2017) Carbon sequestration in an expanded lake system during the Toarcian oceanic anoxic event. *Nature Geoscience* **10**, 129–34.
- Xu W, Ruhl M, Jenkyns HC, Leng MJ, Huggett JM, Minisini D, Ullmann CV, Riding JB, Weijers JW, Storm MS and Percival LM** (2018) Evolution of the Toarcian (Early Jurassic) carbon-cycle and global climatic controls on local sedimentary processes (Cardigan Bay Basin, UK). *Earth and Planetary Science Letters* **484**, 396–411.